3-1-1983

The Effect of Developer Composition on Adjacency Effects in Black and White Photography: Metol vsl Phenidone

Paul L. Zengerle

THE EFFECT OF DEVELOPER COMPOSITION ON ADJACENCY EFFECTS IN BLACK AND WHITE PHOTOGRAPHY: METOL VS. PHENIDONE

by

Paul Leo Zengerle

B.S. University of Windsor

(1975)

A thesis submitted in partial fulfillment
of the requirements for the degree of
Master of Science in the School of
PhotographicArts and Sciences in the
College of Graphic Arts and Photography
of the Rochester Institute of Technology

March, 1983

Signature of the Author Paul Zengerle .....
Photographic Science
and Instrumentation

Accepted by .....
Coordinator, Graduate Program

School of Photographic Arts and Sciences
Rochester Institute of Technology
Rochester, New York

CERTIFICATE OF APPROVAL

MASTER'S THESIS

The Master's Thesis of Paul L. Zengerle
has been examined and approved
by the thesis committee as satisfactory
for the thesis requirement for the
Master of Science degree

.....
Dr. Paul Gilman, Thesis Advisor

.....
Dr. Roland Willis, Thesis Advisor

.....
Dr. Ronald Francis

March 11, 1983
.....
(Date)

THESIS RELEASE PERMISSION FORM

ROCHESTER INSTITUE OF TECHNOLOGY
COLLEGE OF GRAPHIC ARTS AND PHOTOGRAPHY

Title of Thesis THE EFFECT OF DEVELOPER COMPOSITION ON ADJACENCY EFFECTS IN BLACK AND WHITE PHOTOGRAPHY: METOL VS. PHENIDONE

I, Paul Leo Zengerle, hereby grant permission to the Wallace Memorial Library of R.I.T. to reproduce my thesis in whole or in part. Any reproduction will not be for commercial use or profit.

Date _____

ACKNOWLEDGEMENTS

Successful completion of this thesis was only possible because of the technical support and encouragement provided by many individuals:

Dr. Paul Gilman of the Kodak Research Laboratories who kindly consented to act as thesis advisor for this project, and gave much of his time and encouragement in its supervision.

Dr. Roland Willis of the Kodak Research Laboratories who also acted as thesis advisor, and willingly provided a great deal of technical assistance throughout the course of the project.

Mr. Harry Franchino of the Kodak Research Laboratories who provided valuable and timely advice.

Mr. James Snow of the Kodak Research Laboratories who kindly provided his darkroom facilities for this project.

My wife, Carol, who gave much of her time and effort in the preparation of this document.

The Eastman Kodak Company is also gratefully acknowledged for their financial support and the use of Company facilities.

DEDICATION

This thesis is dedicated to
my friend, Carol,
who understandingly accepted
my absence and neglect on
many weekends and evenings
during our first year of marriage

THE EFFECT OF DEVELOPER COMPOSITION ON ADJACENCY EFFECTS IN BLACK AND WHITE PHOTOGRAPHY: METOL VS. PHENIDONE

by

Paul Leo Zengerle

Submitted to the Photographic Science and Instrumentation Division in partial fulfillment of the requirements for the Master of Science degree at the Rochester Institute of Technology

ABSTRACT

Increased chemical adjacency effects in black and white photography can be obtained using certain Metol and Phenidone developers. Four different effects are described:

1) development inhibition by iodide ion
2) development inhibition by bromide ion
3) exhaustion of Metol
4) development inhibition by oxidized Phenidone

Edge effects produced by Metol exhaustion and by Phenidone development are enhanced by moderate increases in pH. They are reduced by: the addition of hydroquinone, high levels of sodium sulfite, and high fog levels.

Developers designed to increase adjacency effects also increase granularity. The trade-off between acutance and granularity is approximately linear for the film-developer combinations studied, with the exception of a Phenidone only developer, which resulted in excessive granularity.

With low-speed films like KODAK Panatomic-X, the sharpness increase observed in photographic prints may be beneficial in spite of increased graininess. However, with higher speed films such as KODAK Plus-X and KODAK Tri-X, the increased grain overwhelms the gain in sharpness, making the trade-off unfavorable.

TABLE OF CONTENTS

I.	Introduction	1
	1. General	1
	2. History	1
	3. Past Studies	2
	4. Research Objective	4
II.	Experimental	5
	1. General	5
	2. Materials	5
	3. Exposure and Processing	6
	4. Analysis of Adjacency Effects	8
	5. Acutance - Granularity Relationship	16
	6. Microscopy	19
III.	Results and Discussion	21
	1. General	21
	2. Metol Developer Variations	23
	a. Metol at 2.0 g/l	25
	b. Metol at 0.2 g/l	35
	3. Phenidone Developer Variations	44
	4. Acutance - Granularity Relationship	56
	a. Objective Evaluation	57
	b. Subjective Evaluation	67
	5. MTF Enhancement with Metol and Phenidone	67
IV.	Conclusions	71
V.	References	73

TABLE OF CONTENTS (Continued)

VI. Appendices 76

1. Appendix A. Calculation of Relative Speed Values 77
2. Appendix B. Normalization Procedure for Comparing Edge Densities 78
3. Appendix C. Calculation of MTF curves and CMT Acutance Values 80
4. Appendix D. RMS Granularity Measurement 84

VII. Vita 86

LIST OF TABLES

Table Number		Page Number
I.	Developer Formulas	10
	1. Developers Used in Initial Survey	10
	2. Metol Concentration Series	11
	3. Sulfite Series with Metol at 2.0 g/l	11
	4. Hydroquinone Series with Metol at 2.0 g/l	12
	5. Developer pH Series with Metol at 2.0 g/l	12
	6. Developer Temperature Series	13
	7. Sulfite Series with Metol at 0.2 g/l	13
	8. Hydroquinone Series with Metol at 0.2 g/l	13
	9. Developer pH Series with Metol at 0.2 g/l	14
	10. Phenidone Concentration Series	14
	11. Sulfite Series with Phenidone at 1.5 g/l	14
	12. Developer pH Series with Phenidone at 1.5 g/l	15
	13. Hydroquinone Series with Phenidone at 1.5 g/l	15
	14. Hydroquinone Series with Phenidone at 0.3 g/l	15
II.	Photographic Data for Various Film - Developer Combinations	58
III.	Analyzed Silver in $g/m^2 \times 10^2$ For Various Film - Developer Combinations at Different Densities	65

LIST OF FIGURES

Figure Number		Page Number
1.	Mechanism for the Formation of Adjacency Effects	3
2.	Method Used to Analyze Adjacency Effects	7
3.	Net Edge Density as a Function of Developer Type	22
4.	Net Edge Density as a Function of Metol Concentration	24
5.	Net Edge Density as a Function of Sulfite Level at 2.0 g/l of Metol	25
6.	Net Edge Density as a Function of Hydroquinone Concentration at 2.0 g/l	26
7.	Net Edge Density as a Function of pH at 2.0 g/l of Metol	27
8.	Electrochemistry of Metol	28
9.	Effect of pH on Development Rate with Metol at 2.0 g/l	29
10.	Adjacency Effects with D-76 versus PZ-16 (pH 11.4) Using Microdensitometer Traces of X-ray Lines	31
11.	Net Edge Density as a Function of Developer Temperature	32
12.	Effect of Temperature on Development Rate with Metol at 2.0 g/l at pH 9.3	32
13.	Comparison of Development and Fog Rates at High Temperature (100°F) and High pH (11.4)	33
14.	Effect of Developer Temperature on Edge Width Using Microdensitometer Traces of X-ray Lines	34
15.	Net Edge Density as a Function of Sulfite Level at 0.2 g/l of Metol	35

LIST OF FIGURES (Continued)

Figure Number		Page Number
16.	Effect of Sulfite Level on the Uninhibited Density with Metol at 0.2 g/l	36
17.	Effect of Sulfite Level on Adjacency Effects at 0.2 g/l of Metol Using Microdensitometer Traces of X-ray Lines.	37
18.	Net Edge Density as a Function of Hydroquinone Concentration at 0.2 g/l of Metol	38
19.	Effect of Hydroquinone on the Development Rate of Low-Metol (0.2 g/l) Developers	39
20.	Net Edge Density as a Function of pH at 0.2 g/l of Metol	40
21.	Effect of pH on Adjacency Effects with Metol at 0.2 g/l Using Microdensitometer Traces of X-ray Lines	41
22.	Summary of Adjacency Effects Produced with Metol Development	42
23.	Comparison of Development Rates with Dilute Metol and Phenidone Developers	44
24.	Net Edge Density as a Function of Phenidone Concentration	45
25.	Net Edge Density as a Function of Sulfite Level at 1.5 g/l of Phenidone	46
26.	Effect of Sulfite Level on the Uninhibited Density with Phenidone at 1.5 g/l	47
27.	Net Edge Density as a Function of pH at 1.5 g/l of Phenidone	48
28.	Net Edge Density as a Function of Hydroquinone Concentration at 1.5 g/l of Phenidone	49

LIST OF FIGURES (Continued)

Figure Number		Page Number
29.	Effect of Hydroquinone on Adjacency Effects with Phenidone Development Using Microdensitometer Traces of X-ray Lines	50
30.	Photomicrographs of developed Tri-X grains for POTA and PZ-143 at matched exposure and density (D_V = 0.34)	51
31.	Effect of Hydroquinone on the Development Rate with Phenidone	53
32.	Effect of Hydroquinone on the Uninhibited Development Rate with Phenidone	54
33.	Summary of Adjacency Effects Produced with Phenidone Development	55
34.	Microdensitometer Traces of X-ray Lines for Various Film - Developer Combinations	59
35.	MTF curves for D-76, PZ-143, PZ-21, and POTA with KODAK Panatomic-X Film	60
36.	MTF curves for D-76, PZ-143, PZ-21, and POTA with KODAK Plus-X Film	61
37.	MTF curves for D-76, PZ-143, PZ-21, and POTA with KODAK Tri-X Film	62
38.	CMT Acutance versus Gamma-Normalized RMS Granularity for the Various Film - Developer Combinations	63
39.	Photomicrographs of the developed silver image obtained with KODAK Tri-X Film with POTA versus PZ-143 at matched exposure and densities (D_V = 0.93)	66
40.	Schematic Illustration of Low-Frequency MTF Enhancement with Low-Metol Developers	68
41.	Schematic Illustration of No High-Frequency MTF Enhancement with Low-Metol Developers	69

LIST OF FIGURES (Continued)

Figure Number		Page Number
42.	Schematic Illustration of High - Frequency MTF Enhancement with POTA	69
43.	Method Used to Calculate Relative Speed Values	77
44.	Edge Density Normalization Procedure	79
45.	Sine-wave exposure on a negative working film	80
46.	A microdensitometer trace of KODAK Tri-X Film	84
47.	KODAK Panatomic-X Film - D-76 Developer	87
48.	KODAK Panatomic-X Film - PZ-143 Developer	88
49.	KODAK Panatomic-X Film - PZ-21 Developer	89
50.	KODAK Panatomic-X Film - POTA Developer	90
51.	KODAK Plus-X Film - D-76 Developer	91
52.	KODAK Plus-X Film - PZ-143 Developer	92
53.	KODAK Plus-X Film - PZ-21 Developer	93
54.	KODAK Plus-X Film - POTA Developer	94
55.	KODAK Tri-X Film - D-76 Developer	95
56.	KODAK Tri-X Film - PZ-143 Developer	96
57.	KODAK Tri-X Film - PZ-21 Developer	97
58.	KODAK Tri-X Film - POTA Developer	98

INTRODUCTION

1) General

Picture sharpness is influenced by development effects, which cause a change in the density of the photographic image at the sharp boundary between areas of high and low exposure.[1] These effects, often called adjacency effects, are caused by local chemical changes in the developer during the development period, and may either restrain or enhance the amount of silver image that may normally be formed.[2]

Sharpness is one of the impressions a human being gets when observing the detail in a photographic image.[3] This impression is influenced by the density difference of the image at the boundary of a light and dark area.[4] Increases in density on the edges of detail by adjacency effects can enhance this visual impression, resulting in images with improved definition.[5]

2) History

Developer adjacency effects in photography have been known for many years. They are also referred to as "edge effects", "development effects", "fringe and border effects", and "neighborhood effects".[6,7,8]

They were probably first recognized by Alexander Mackie in 1885.[9] His work, as well as others, gave rise to the term "Mackie Line", referring to the white outline produced by these development effects.[10,11,12]

Another early contributor in this field was Gustav Eberhard, who studied a particular consequence of adjacency effects. Eberhard found that the density of the developed image was often related to its size.[13] Small images were found to have higher densities than large ones, even though both areas had the same exposure and development.[14] This became known as the Eberhard effect.[15]

3) Past Studies

Several different types of adjacency effects have been described. Certain edge effects are associated with lack of agitation of the developing solution, but this often results in mottled, non-uniform image development.[16,17] In addition, these effects are often too gross in character to be of any benefit. Several investigators have studied the effect of using silver halide solvents in the developer to modify the developed image structure, which often results in speed losses and increased silver consumption.[18,19,20] Since these methods have inherent disadvantages and have already received considerable attention in the literature, they are not included in this investigation.

Many efforts have been made to compound developers that use edge effects benefically to give increased edge contrast to yield pictures with improved sharpness. In general, high-acutance developers discussed in the literature are of the one-use type described by Beutler.[21] These are developers containing very low levels of Metol and sodium sulfite along with adequate alkali to obtain active development.[22] The Metol concentration is kept low, so that the developing agent will be exhausted rapidly in the highly exposed areas of the film.[23] It is also presumed that in areas of highly active development, the pH of the developer there may be somewhat lower due to the rapid formation of acid products released during development.[24] Active developer diffusing from areas of low to high exposure as well as development inhibiting by-products (halide ion, oxidized developer, etc.) diffusing in the opposite direction result in increased development of the boundary of the image.[25] This general description of the mechanism by which adjacency effects are formed is illustrated in Figure 1.

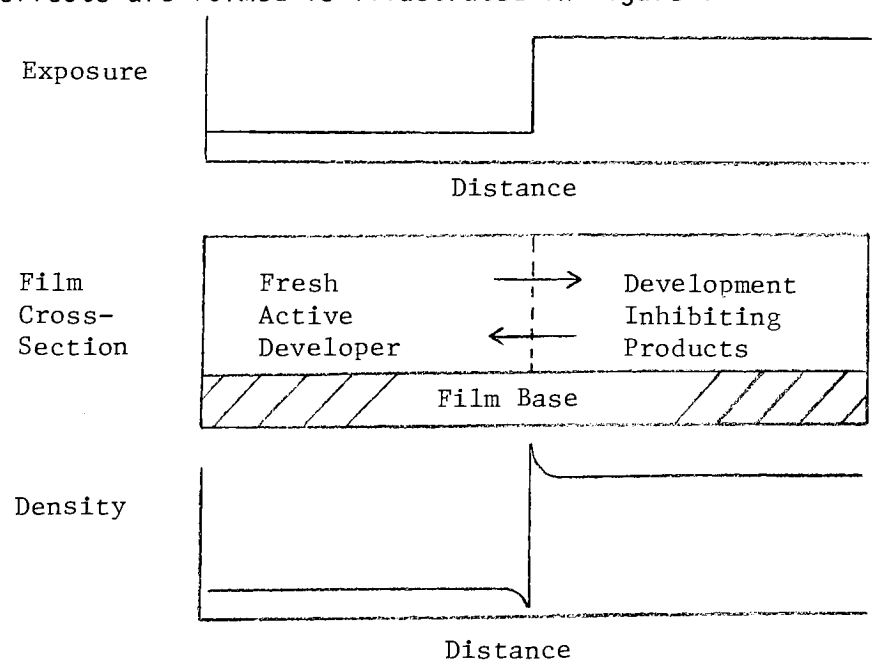

Figure 1 - Mechanism for the Formation of Adjacency Effects.

Formulas for high-acutance developers are optimized to favor the formation of development edge effects. However, developers designed to utilize edge effects to improve image definition do so at the expense of increasing the graininess of the image.[26] Hence, high-acutance developers are usually used with fine-grain photographic films of low or moderate speed.[27] Generally, a high price must be paid in granularity in order to achieve a moderate gain in acutance with these developers. However, the sharpness improvement may be worthwhile if the system is grain-limited by the film emulsion.[28]

4) Research Objective

Even though adjacency effects are well-known and have received considerable attention in the literature, a comprehensive investigation of these effects is lacking. The purpose of this study is to determine systematically the properties of a developer that have a significant influence on adjacency effects. Specifically, such properties include: developing agent type and concentration, sodium sulfite level, developer pH, and the use of superadditive developing agents. In addition, the mechanisms by which these properties alter adjacency effects and the nature of the development inhibiting products involved are also described. Finally, the acutance-granularity trade-off that exists with these developers is quantified and illustrated using definition pictures.

EXPERIMENTAL

1) General

All experimental work was carried out at the Kodak Research Laboratories. Chemicals used for these experiments were of photographic grade or higher.

2) Materials

KODAK Tri-X Pan Film 5063 was used as the photographic material to study the influence of developer composition on adjacency effects. It was chosen because it is capable of producing edge effects of high magnitude, which are sensitive to variations in developer formulation, and exhibits noticeable differences when changes in granularity occur.

KODAK Panatomic-X Pan 5060 and KODAK Plus-X Pan 5062, as well as Tri-X 5063 were used in the experiments comparing acutance versus granularity.

3) Exposure and Processing

An Eastman Intensity Scale Automatic Model IV I-B sensitometer provided a stepped exposure (0-6, 2 sec., 2850^{o}K, D/LV Filter) to determine relative values for speed, fog, and contrast index. An arbitrary speed point (0.20 density above base plus fog) was used to assign relative speed values as described in Appendix A. Contrast index was determined by the method given in KODAK Publication No. F-5. An Eastman KODAK Model R297 multiple slit X-ray sensitometer provided X-ray line exposures (16 kilovolts, 12 milliamps) of variable time (1/2, 1, 2, 4, and 8 sec.) and width (10μ, 1000μ), which were used as non-scattering radiation to produce edges. A time of development series for both types of exposure was then obtained for each experimental developer.

All developers were made up immediately prior to processing. The developer pH was measured and/or adjusted at 70^{o}F using a Leeds and Northrup (CAT 7664) pH meter. The 12 inch, 35mm film strips were processed vertically in 2 liter deep tanks on film racks with the heavily exposed end toward the bottom of the tank for both types of exposure. The development temperature was 70^{o}F. Intermittent nitrogen burst agitation (for 2 sec. of every 10 sec.) was used to obtain uniform, reproducable development and eliminate development drag effects as much as possible.

The following processing sequence was used:

Developer	X min
KODAK SB-5a Stop Bath	30 sec.
KODAK Rapid Fixer	3 min.
Running Water Wash	5 min.
KODAK Photo-Flo	30 sec.

The experimental data reported in this thesis is based on an average of two runs, unless otherwise stated.

A KODAK Model III densitometer employing a visual readout filter was used to obtain D-log E curves from the processed I-B sensitometric strips. A KODAK Model III microdensitometer was used to measure the edge and macro densities of the processed X-ray lines. The lines used for these comparisions correspond to an exposure just off of the shoulder of the D-log E curve, as shown in Figure 2 (a). This was chosen because it is a relatively highly exposed area where a considerable amount of development inhibiting products will be formed, yet below Dmax allowing for reasonable edge enhancement. This was determined experimentally to be a 4 second X-ray exposure at the previously stated current and voltage.

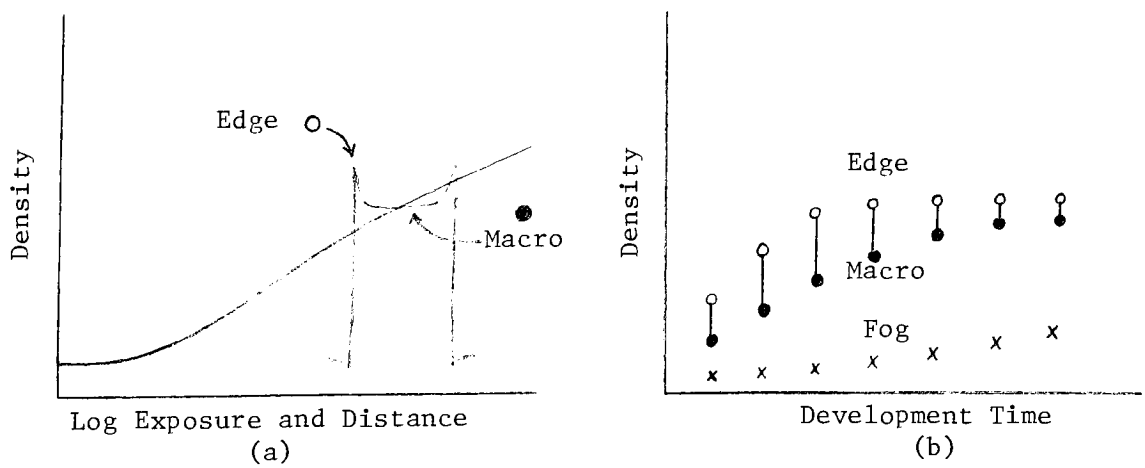

Figure 2 - Method Used to Analyze Adjacency Effects

4) Analysis of Adjacency Effects

The initial approach to this project was to survey several known developers. These were chosen to encompass different developing agents as well as provide a wide range of development rates. All developer formulations used are given in Table I at the end of this section.

Plots of edge density and macro density (both obtained from the 1000μ X-ray line) and fog versus development time were used to study edge effects as a function of development rate, as illustrated in Figure 2(b). The maximum separation between edge density and macro density at any development time, was used as a criterion for determining the magnitude of the adjacency effects. Due to development "drag effects", the X-ray line positioned lower in the tank was often of lower density than the other edge. The edge with higher density (positioned higher in the tank) was used in this procedure. Generally, this maximum separation occurs at a development time which yields a useful value for contrast index. Since edge height varies with macro density for a given X-ray line exposure and developer, comparisons among developers with regard to edge height are only valid at equal macro densities. For this reason, a normalization procedure was used to compare edge effects among different developers when exactly equal macro densities were not obtained. A macro density value of 1.50 was chosen for the purpose of illustrating data. This represents approximately half of the uninhibited density given by the 10μ X-ray line data, allowing the formation of high adjacency effects.

It is emphasized, however, that the trends indicated by the data were evident over a wide range of macro densities by the density-development time plots. The difference between the edge density and macro density is referred to as the "net edge density". The normalization procedure is described in Appendix B. The 10μ X-ray line is used to give the density produced in the absence of any development inhibition.

TABLE I

Developer Formulas

Ingredients are given in grams/liter and pH measurements are made at 70 F unless otherwise stated. In some cases, identical formulas may appear under different names.

1) Developers Used in Initial Survey

KODAK D-76[29]

Metol	2.0	
Sodium Sulfite	100.0	
Hydroquinone	5.0	
Borax	2.0	
H_2O to	1.0	l
pH =	8.6	

KODAK D-11[30]

Metol	1.0	
Sodium Sulfite	75.0	
Hydroquinone	9.0	
Sodium Carbonate	30.0	
Potassium Bromide	5.0	
H_2O to	1.0	l
pH =	9.8	

KODAK D-8[31]

Sodium Sulfite	90.0	
Hydroquinone	45.0	
Sodium Hydroxide	37.5	
Potassium Bromide	30.0	
H_2O to	1.0	l
pH =	13.0	

Beutler[32]

Metol	1.0	
Sodium Sulfite	5.0	
Sodium Carbonate	5.0	
H_2O to	1.0	l
pH =	10.1	

Purdon[33]			POTA[34]		
Sodium Sulfite	75.0		Phenidone	1.5	
p-Phenylenediamine	10.0		Sodium Sulfite	30.0	
10% Ammonium Carbonate (cc/l)	5.0		H_2O to	1.0	l
H_2O to	1.0	l	pH =	8.6	
pH =	9.3				

2) Metol Concentration Series

	PZ-21		PZ-22		PZ-23		PZ-24	
Metol	0.2		0.5		1.0		2.0	
Sodium Sulfite	2.0		2.0		2.0		2.0	
Borax	1.5		3.0		5.0		7.5	
H_2O to	1.0	l	1.0	l	1.0	l	1.0	l
pH =	8.6		8.6		8.6		8.6	

3) Sulfite Series with Metol at 2.0 g/l

	PZ-1*		PZ-2		PZ-3		PZ-4	
Metol	2.0		2.0		2.0		2.0	
Sodium Sulfite	0.0		2.0		30.0		100.0	
Borax	7.5		7.5		2.0		0.0	
H_2O to	1.0	l	1.0	l	1.0	l	1.0	l
pH =	8.6		8.6		8.6		8.6	

4) Hydroquinone Series with Metol at 2.0 g/l

	PZ-31	PZ-32	PZ-33	PZ-34
Metol	2.0	2.0	2.0	2.0
Sodium Sulfite	2.0	2.0	2.0	2.0
Hydroquinone	0.0	2.0	5.0	20.0
Borax	7.5	10.0	10.0	10.0
H_2O to	1.0 l	1.0 l	1.0 l	1.0 l
pH =	8.6	8.6	8.6	8.6

5) Developer pH Series with Metol at 2.0 g/l

	PZ-11	PZ-12	PZ-13	PZ-14	PZ-15	PZ-16
Metol	2.0	2.0	2.0	2.0	2.0	2.0
Sodium Sulfite	2.0	2.0	2.0	2.0	2.0	2.0
Borax	2.0	7.5	0.0	0.0	0.0	0.0
Sodium Carbonate	0.0	0.0	2.0	10.0	10.0	10.0
1.0N Sodium Hydroxide	0.0	0.0	0.0	0.0	10.0	31.0
H_2O to	1.0 l	1.0 l	1.0 l	1.0 l	1.0 l	1.0 l
pH =	7.7	8.6	9.3	10.2	10.8	11.4

6) Developer Temperature Series

	PZ-13	PZ-13A	PZ-13B	PZ-13C
Metol	2.0	2.0	2.0	2.0
Sodium Sulfite	2.0	2.0	2.0	2.0
Sodium Carbonate	2.0	2.0	2.0	2.0
H_2O to	1.0 l	1.0 l	1.0 l	1.0 l
Temp. (^oF)	70^oF	80^oF	90^oF	100^oF
pH @ above temp.	9.3	9.5	9.7	9.8

7) Sulfite Series with Metol at 0.2 g/l

	PZ-41	PZ-42	PZ-43**
Metol	0.2	0.2	0.2
Sodium Sulfite	2.0	30.0	100.0
Borax	1.5	0.0	0.0
H_2O to	1.0 l	1.0 l	1.0 l
pH =	8.6	8.6	8.6

8) Hydroquinone Series with Metol at 0.2 g/l

	PZ-71	PZ-72	PZ-73	PZ-74
Metol	0.2	0.2	0.2	0.2
Sodium Sulfite	2.0	2.0	2.0	2.0
Hydroquinone	0.0	2.0	5.0	20.0
Borax	1.5	2.0	3.0	12.0
H_2O to	1.0 l	1.0 l	1.0 l	1.0 l
pH =	8.6	8.6	8.6	8.6

9) Developer pH Series with Metol at 0.2 g/l

	PZ-61	PZ-62	PZ-63	PZ-64
Metol	0.2	0.2	0.2	0.2
Sodium Sulfite	2.0	2.0	2.0	2.0
Borax	7.5	0.0	0.0	0.0
Sodium Carbonate	0.0	0.3	3.0	10.0
1.0N Sodium Hydroxide (cc/l)	0.0	0.0	0.0	15.0
H_2O to	1.0 l	1.0 l	1.0 l	1.0 l
pH =	8.6	9.6	10.6	11.6

10) Phenidone Concentration Series

	PZ-101**	PZ-102**	PZ-103	PZ-104+
Phenidone	0.3	0.75	1.5	4.5
Sodium Sulfite	30.0	30.0	30.0	30.0
H_2O to	1.0 l	1.0 l	1.0 l	1.0 l
pH =	8.6	8.6	8.6	8.6

11) Sulfite Series with Phenidone at 1.5 g/l

	PZ-111 *	PZ-112	PZ-113	PZ-114
Phenidone	1.5	1.5	1.5	1.5
Sodium Sulfite	0.0	2.0	30.0	100.0
Borax	5.0	1.5	0.0	0.0
H_2O to	1.0 l	1.0 l	1.0 l	1.0 l
pH =	8.6	8.6	8.6	8.6

12) Developer pH Series with Phenidone at 1.5 g/l

	PZ-131	PZ-132	PZ-133	PZ-134
Phenidone	1.5	1.5	1.5	1.5
Sodium Sulfite	30.0	30.0	30.0	30.0
Sodium Carbonate	0.0	1.6	5.0	5.0
1.0N Sodium Hydroxide (cc/l)	0.0	0.0	7.0	22.0
H_2O to	1.0 l	1.0 l	1.0 l	1.0 l
pH =	8.6	9.6	10.6	11.6

13) Hydroquinone Series with Phenidone at 1.5 g/l

	PZ-121	PZ-122**	PZ-123**
Phenidone	1.5	1.5	1.5
Sodium Sulfite	30.0	30.0	30.0
Hydroquinone	0.0	5.0	20.0
H_2O to	1.0 l	1.0 l	1.0 l
pH =	8.6	8.6	8.6

14) Hydroquinone Series with Phenidone at 0.3 g/l

	PZ-141+	PZ-142+	PZ-143	PZ-144**
Phenidone	0.3	0.3	0.3	0.3
Sodium Sulfite	30.0	30.0	30.0	30.0
Hydroquinone	0.0	2.0	5.0	20.0
H_2O to	1.0 l	1.0 l	1.0 l	1.0 l
pH =	8.6	8.6	8.6	8.6

* Prepared under bubbling N_2.
** pH reduced using concentrated sulfuric acid.
+ pH increased using 1.0N sodium hydroxide.

5) Acutance - Granularity Relationship

The trade-off between acutance and granularity with certain high-acutance developers was studied with three forenamed films. The following developers provided different situations for the formation of edge effects:

D-76 - a Metol-hydroquinone developer
PZ-143 - a Phenidone-hydroquinone developer
PZ-21 - a low-Metol developer
POTA - a Phenidone developer

In this study, modulation transfer function curves and corresponding CMT acutance values were used as the objective correlate of sharpness, since they have been shown to give a consistent ranking of films having a large amount of chemical adjacency effects.[35] These measurements were obtained from the Materials Coating and Engineering Division of the Kodak Research Laboratories. They were made by exposing the film using a target which consists of a series of sine wave patterns of increasing frequency. Exposure conditions were chosen to achieve a mid-scale density on the corresponding D-log E curve. A 35% modulation target was used with the following exposures:

Film	Exposure Time	Filter
KODAK Panatomic - X	1/30 sec.	--
KODAK Plus-X	1/30 sec.	0.50 N.D.
KODAK Tri-X	1/15 sec.	1.20 N.D.

The resulting density profile of the processed film strips is the physical quantity that is measured. A detailed discussion of the method used to obtain the MTF measurements and CMT values is given in Appendix C.[36,37]

RMS granularity measurements were used as the objective correlate of graininess. These were obtained from the Film Technical Services Division of Kodak Park. A 48 μ scanning aperture was used. The 35mm film strips were given a I-B sensitometric exposure using a 0-3 wide-step (20mm) tablet. A thin ground-glass plate was placed below the step tablet to achieve a diffuse exposure. The following exposure conditions were used:

Film	Exposure
KODAK Panatomic-X	2 sec., 2850°K, D/LV, 1.2 N.D.
KODAK Plus-X	2 sec., 2850°K, D/LV, 1.6 N.D.
KODAK Tri-X	2 sec., 2850°K, D/LV, 2.0 N.D.

The root mean square granularity σ_D , was then obtained by the method described in Appendix D.[38]

Gamma-normalized granularity was then obtained by dividing σ_D by the instantaneous gamma at that density (or exposure). This corrects for any differences in the measured granularity due to differences in contrast index and/or curve shape.[39] However, it is emphasized that the results obtained without gamma-normalization were essentially the same, since the contrast

indices were closely matched. Granularity comparisons were made at equivalent exposures (yielding a mid-scale density), where the number of latent image centers formed per unit area is the same for a given film. Comparisons of CMT values with RMS granularity measurements were made at the same exposure and magnification (12X).

Definition pictures were also obtained at nearly matched contrast indices for these film-developer combinations to illustrate grain-sharpness trade-offs. A picture scene was chosen to include considerable detail to accentuate image sharpness as well as several uniform areas for accessing the graininess of the image. A target consisting of such a scene was provided by D. M. Zwick.[40]

Negative exposures were provided by the Materials Coatings and Engineering Division of the Kodak Research Laboratories using a definition camera at 8X reduction. A focus series was used to arrive at the optimum position. The following exposure conditions were used:

Film	Exposure Time	Filter
KODAK Panatomic-X	1/200, 1/100, 1/50, 1/25, 1/10, 1/5 sec.	D/LV, 0.20 N.D.
KODAK Plus-X	1/200, 1/100, 1/50, 1/25, 1/10, 1/5 sec.	D/LV, 0.70 N.D.
KODAK Tri-X	1/200, 1/100, 1/50, 1/25, 1/10, 1/5 sec.	D/LV, 1.20 N.D.

The correctly exposed negative was chosen as the one in which the image of the black card on the target (a very lightly exposed area on the negative) was just above base plus fog density.

These negatives were then printed with a Devere 504 color enlarger onto KODAK Ektamatic RC paper at 12X magnification. Exposure times varied between 90 sec. and 150 sec. at f/8. A 0.10 M color filter was used to obtain a print gamma of approximately unity. The original prints were exposed such that the reflection density of the uniform gray background falls between 0.90 and 1.00. The exposed photographic paper was first given a stabilization process with a KODAK Model 214-K Ektamatic Processor which uses KODAK S-II Activator and KODAK Ektamatic S-30 Stabilizer. The prints were subsequently F-5 fixed for 5 minutes, washing with running water at 70^{o}F for 20 minutes, and air dried.

6) Microscopy

Photomicrographs were made using a Zeiss Photomicroscope III with either a 40X (1.00 N.A.) or 100X (1.25 N.A.) oil immersion objective yielding a magnification of 600X or 1500X, respectively. Film samples were mounted emulsion side up on 1mm glass microscope slides using 3M CA-8 Cyanoacrylate

Adhesive. The condenser aperture iris was set so that approximately 2/3 of the objective was used to achieve a good compromise between contrast and resolution. Image resolution is limited to about 0.3μ. A green filter (WR61) was used to minimize chromatic aberration. Original photomicrographs were taken on Type 52 Polaroid film.

RESULTS AND DISCUSSION

1) General

Preliminary work in this area involved the examination of various developers to determine the magnitude of adjacency effects produced with these solutions. The developers chosen for this initial study encompass four developing agents as well as two superadditive developers. It was also expected that these developers would yield widely varying rates of development. Only solutions with published formulas were used. These are given in Table I of the experimental section.

Based on the method used to determine edge effect magnitude described previously, the greatest adjacency effects were produced with POTA and the Beutler formula. KODAK D-76 and KODAK D-11 gave intermediate results, while the Purdon formula and KODAK D-8 yielded the lowest adjacency effects. These results are summarized in Figure 3.

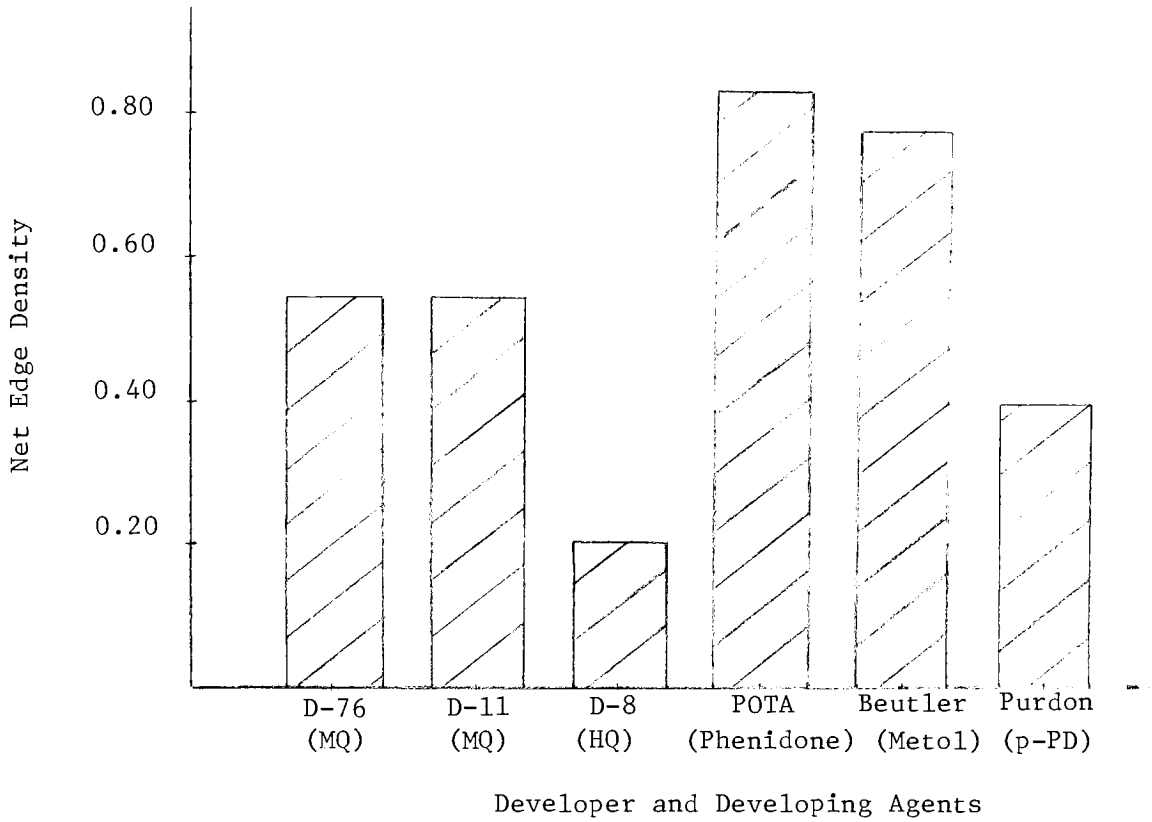

Figure 3 - Net Edge Density as a Function of Developer Type.

It is evident from these data that adjacency effects varied considerably depending on the developing solution used. It is also apparent that solutions employing either Metol (N-methyl-p-aminophenol sulfate) or Phenidone (1-phenyl-3-pyrazolidone) as the sole developing agent produced significantly greater adjacency effects than combinations as in D-76. The results of this brief initial study as well as previous knowledge gained from the literature caused this project to be focused on developers containing these two developing agents.[41]

2) Metol Developer Variations

Developer variations using Metol as the developing agent were based on the following formulas:

	PZ-2	PZ-21
Metol	2.0 g/l	0.2 g/l
Sodium Sulfite	2.0 g/l	2.0 g/l
Borax	7.5 g/l	1.5 g/l
H_2O to	1 liter	1 liter
pH =	8.6	8.6

These developers were designed based on results obtained with D-76 and the Beutler formula. The sodium sulfite level was kept low to minimize any possible reaction with oxidized developing agent as well as reduce any silver halide solvent action. The pH is low enough so that hydroquinone would not be an active developing agent when it is introduced as a variable.[42] The effect of Metol concentration on adjacency effects under these conditions is illustrated in Figure 4.

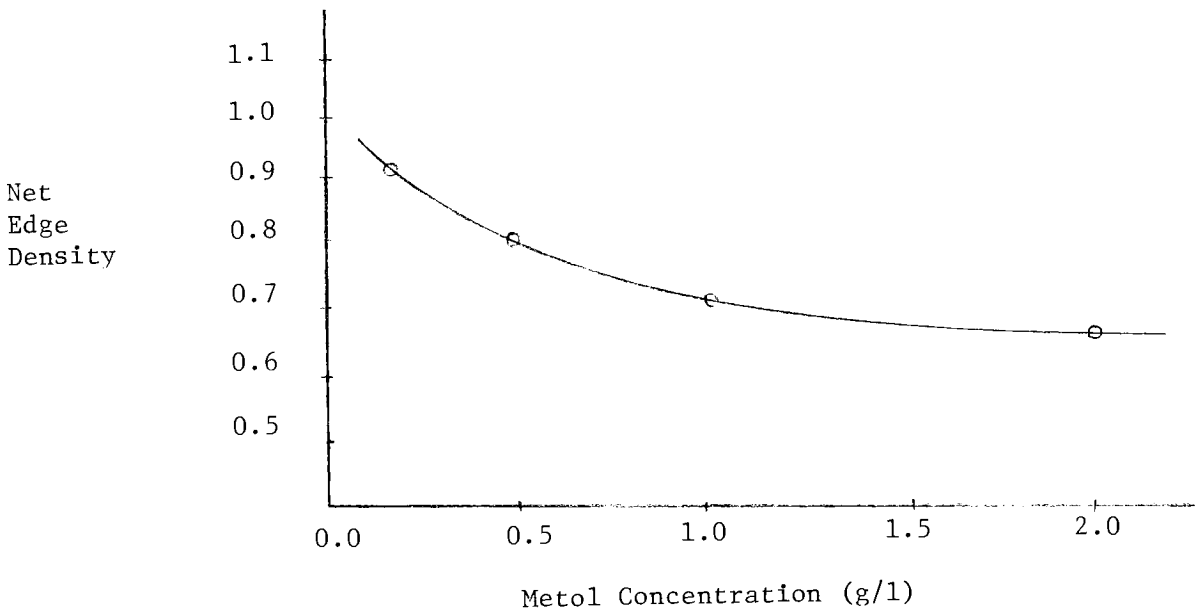

Figure 4 - Net Edge Density as a Function of Metol Concentration.

A consistent trend toward higher adjacency effects is seen as the Metol level is decreased. This behavior is discussed in the literature[43,44], and is attributed to exhaustion of the developing agent as discussed earlier. Since drastically different behavior is observed with Metol depending on the level used, it was studied at two concentrations.

2(a) Metol at 2.0 g/l

Only moderate edge effects were observed when Metol is at a concentration of 2.0 g/l. Figure 5 shows the result of adding sodium sulfite to the developer at this Metol level. No significant change in the magnitude of the adjacency effects was observed. A similar plot for the addition of hydroquinone is shown in Figure 6, and again no difference was observed. Even the combination of hydroquinone (at 5.0 g/l) and a high level of sodium sulfite (100.0 g/l) produced little change in edge density. This is evident from the result obtained from D-76 (see Figure 3). Past studies[45] have shown that oxidized Metol is a development inhibitor which reacts with sodium sulfite and hydroquinone.

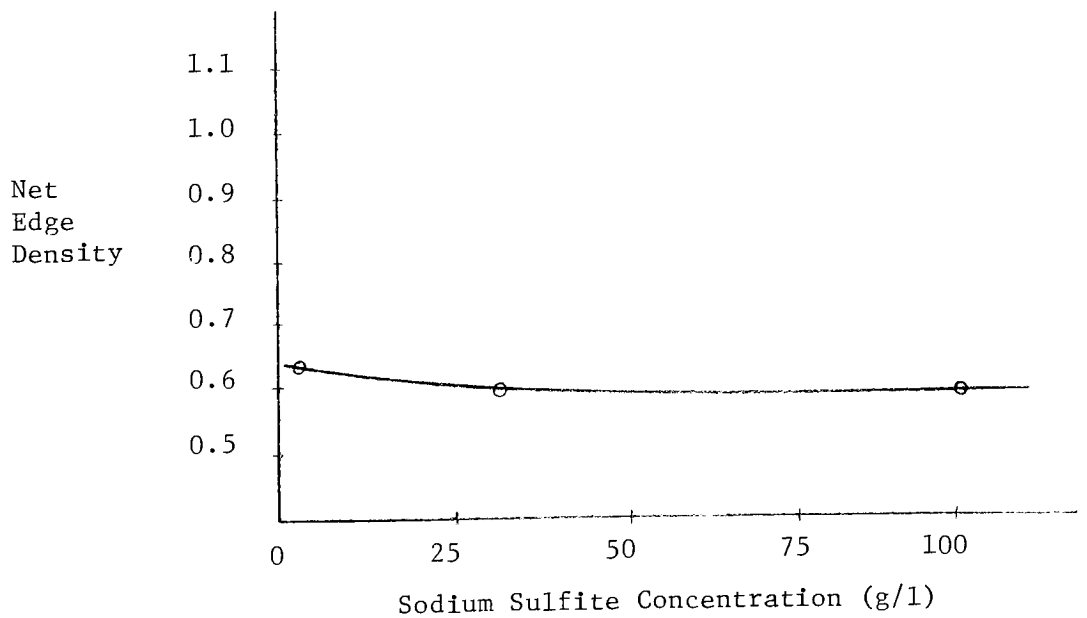

Figure 5 - Net Edge Density as a Function of Sulfite Level at 2.0 g/l of Metol.

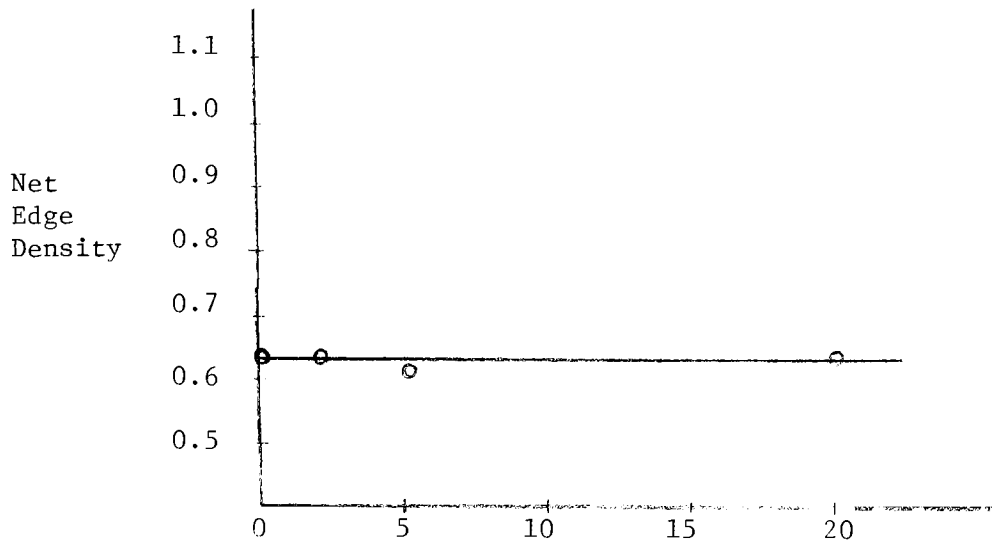

Figure 6 - Net Edge Density as a Function of Hydroquinone Concentration at 2.0 g/l of Metol.

These data indicate that addition of either sulfite or hydroquinone has little bearing on adjacency effect magnitude. Hence, these results imply that oxidized Metol is not involved, and the adjacency effects produced under these conditions are likely due to development inhibition from halide ion released during development.

The effect of developer pH at this Metol level was also investigated. It can be seen from the results depicted in Figure 7 that edge effects increase significantly above pH 10.0.

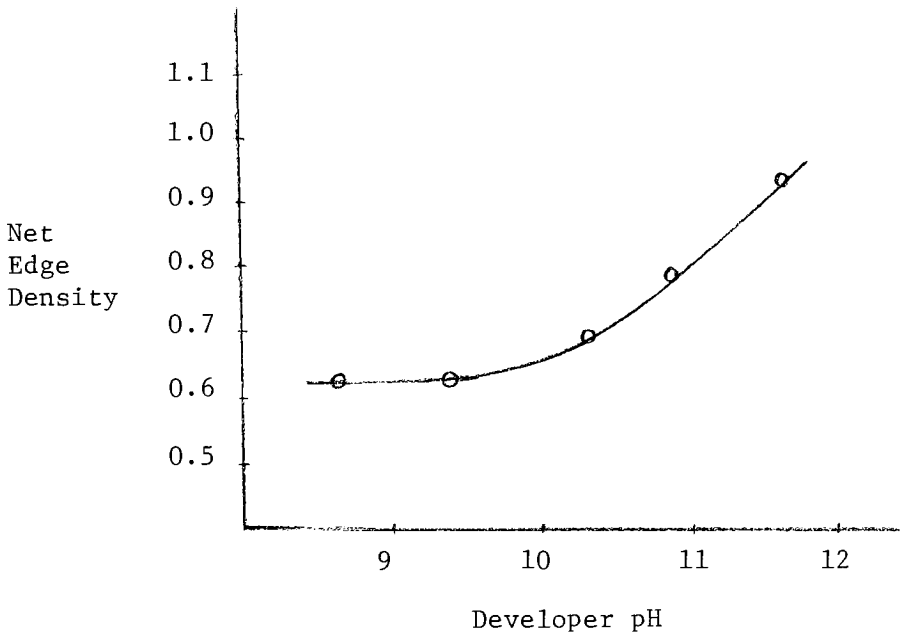

Figure 7 - Net Edge Density as a Function of pH at 2.0 g/l of Metol.

In search of some rationale for this behavior, the electrochemistry of Metol was examined.[46] Electrochemical changes for Metol and its oxidized form as a function of pH are summarized in Figure 8.

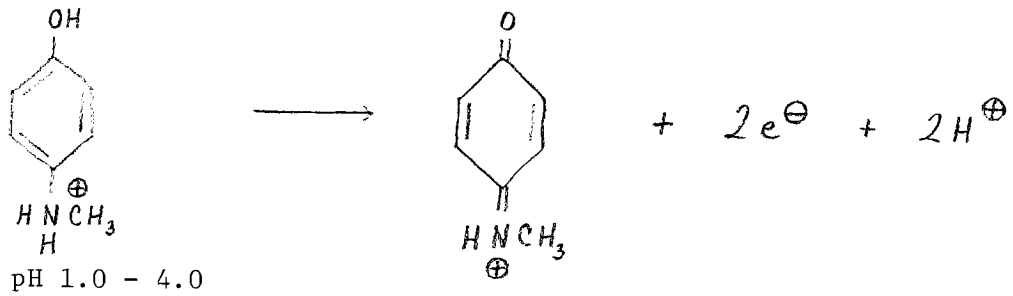

pH 1.0 - 4.0

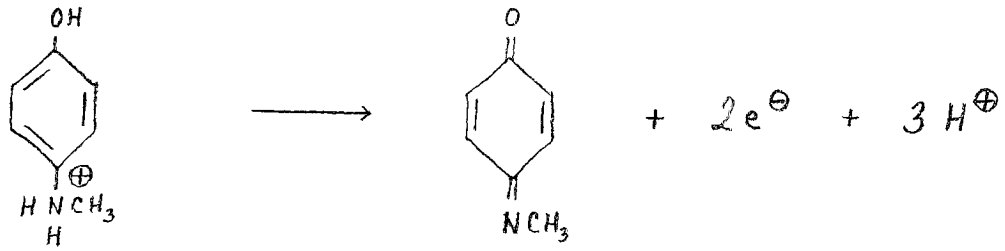

pH 4.0 - 5.75

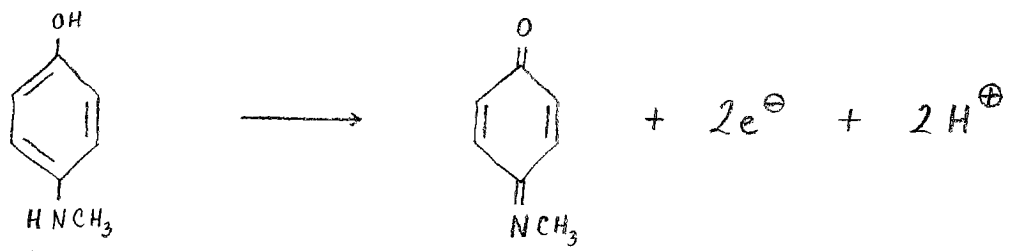

pH 5.75 - 10.3

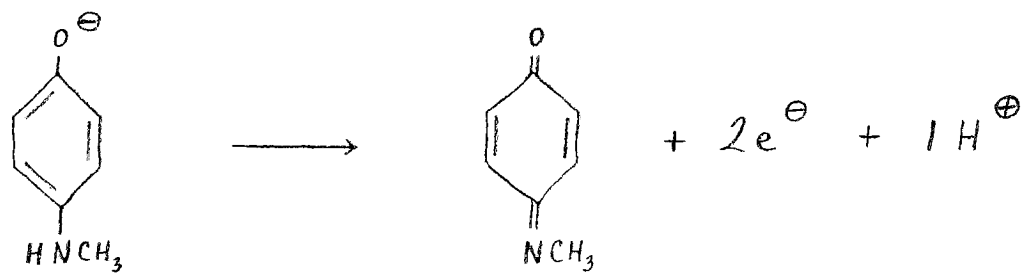

pH 10.3 ⟶

Figure 8 - Electrochemistry of Metol.

From these data, it can be seen that the only change in the region of interest (around pH 10.0) is the loss of a proton from the reduced form at pH 10.3. The only change in the oxidized form occurs at pH 4.0. Hence, there is no change in the oxidized form in the region of interest which might affect development inhibition.

Since the comparisons in Figure 7 are made at matched macro densities and the oxidized form of Metol does not change, we can assume that the same amount of developing inhibiting products as well as the same products are formed. However, the rate of formation of these products is increased as the pH rises, as illustrated in Figure 9.

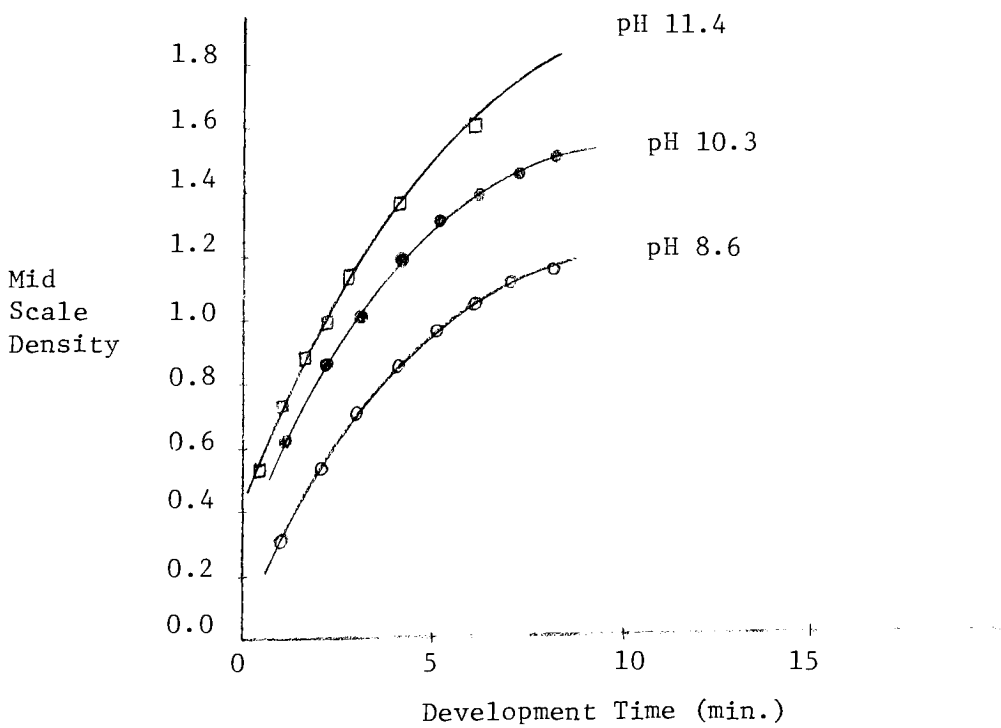

Figure 9 - Effect of pH on Development Rate with Metol at 2.0 g/l.

This suggests that at high pH, the effect of a more diffusable inhibiting species was being observed. The effect of this more diffusable inhibitor would likely go unnoticed at longer development times (lower pH), since it has more time to diffuse out of the film. These high pH edge effects are only slightly reduced with 100.0 g/l of sodium sulfite in the developer. This observation as well as previous experiments suggest that oxidized Metol is not involved in this instance either. Other possibilities include bromide ion and iodide ion. Since the solubility product for silver iodide (Ksp at $25^{o}C$ = 1.5 x $10^{-16}M$) is much lower than that of silver bromide (Ksp at $25^{o}C$ = 7.7 x $10^{-13}M$), iodide ion released during development will tend to adsorb to neighboring emulsion grains, thus inhibiting development there. Bromide ion, on the other hand, will diffuse through the silver bromoiodide matrix unimpeded. However, at high pH, development occurs in a much shorter time period, this period being shorter than the time necessary for much of the bromide ion to diffuse out of the film. Hence, it is plausible that, at high pH, development inhibition by bromide ion is being observed.[47]

A comparison of high pH adjacency effects with those obtained with D-76 at approximately matched macro densities is illustrated in Figure 10.

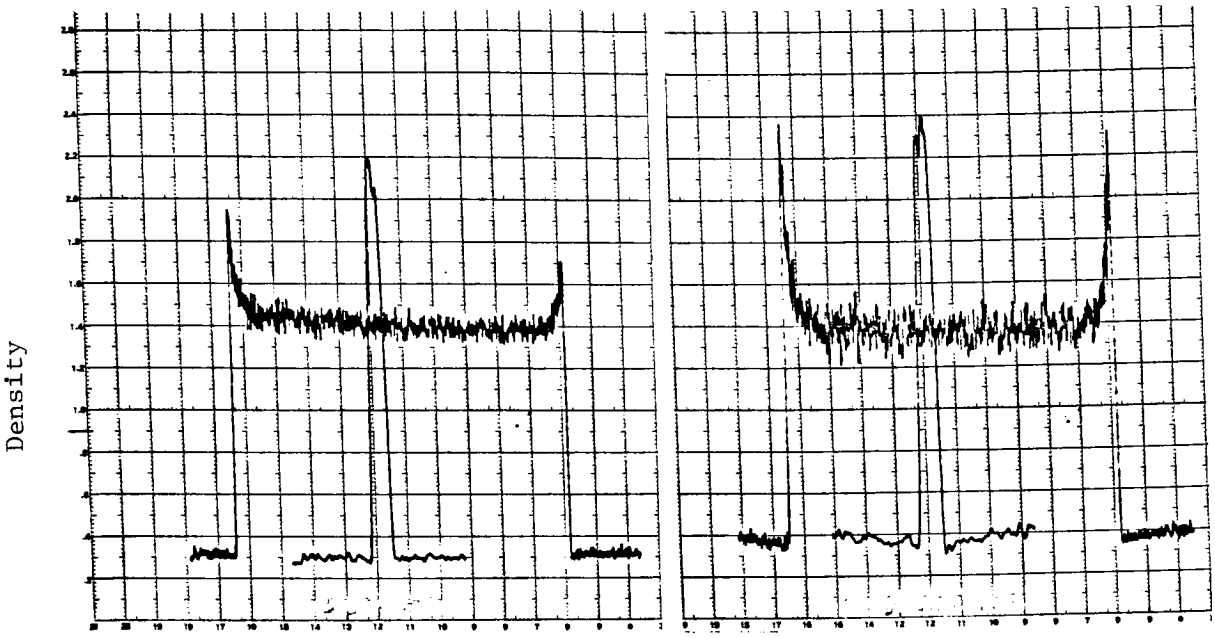

Figure 10 - Adjacency Effects with D-76 versus PZ-16 (pH 11.4) Using Microdensitometer Traces of X-ray Lines.

To further demonstrate that these increased edge effects are indeed a rate phenomena, a pH 9.3 developer (PZ-13) was employed at higher process temperatures to accelerate the rate of development. The developer pH increased slightly with temperature (pH 9.8 at 100°F). Figure 11 shows that edge effects also increase with process temperature (development rate) as seen with increasing pH.

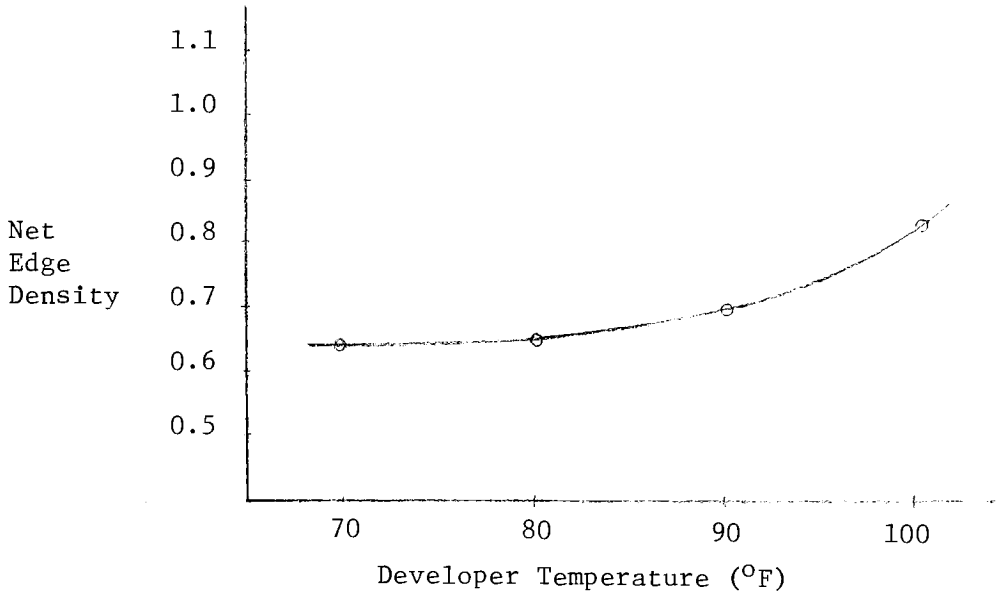

Figure 11 - Net Edge Density as a Function of Developer Temperature.

The effect of temperature on the development rate is shown in Figure 12.

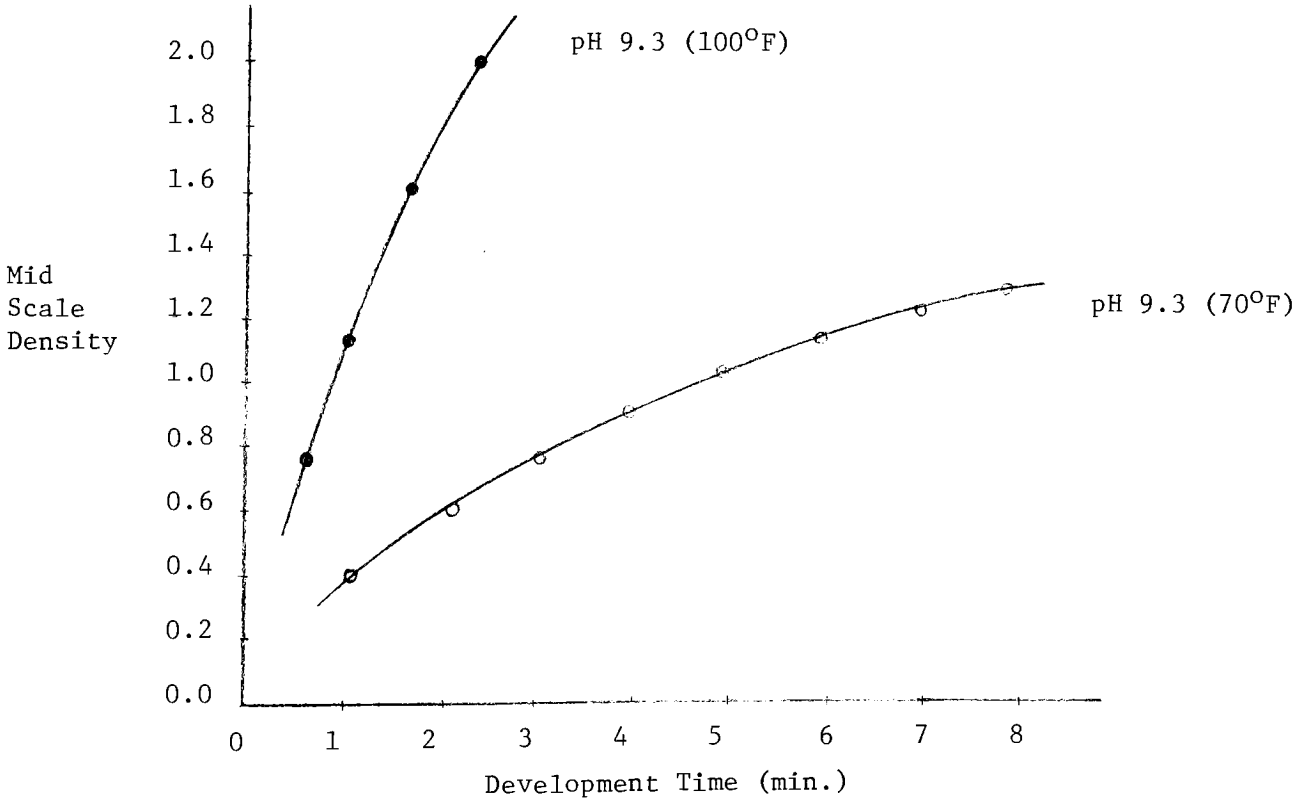

Figure 12 - Effect of Temperature on Development Rate with Metol at 2.0 g/l at pH 9.3.

The development rate at pH 9.3 and 100°F is considerably more rapid than the rate at pH 11.4 and 70°F, as shown in Figure 13.

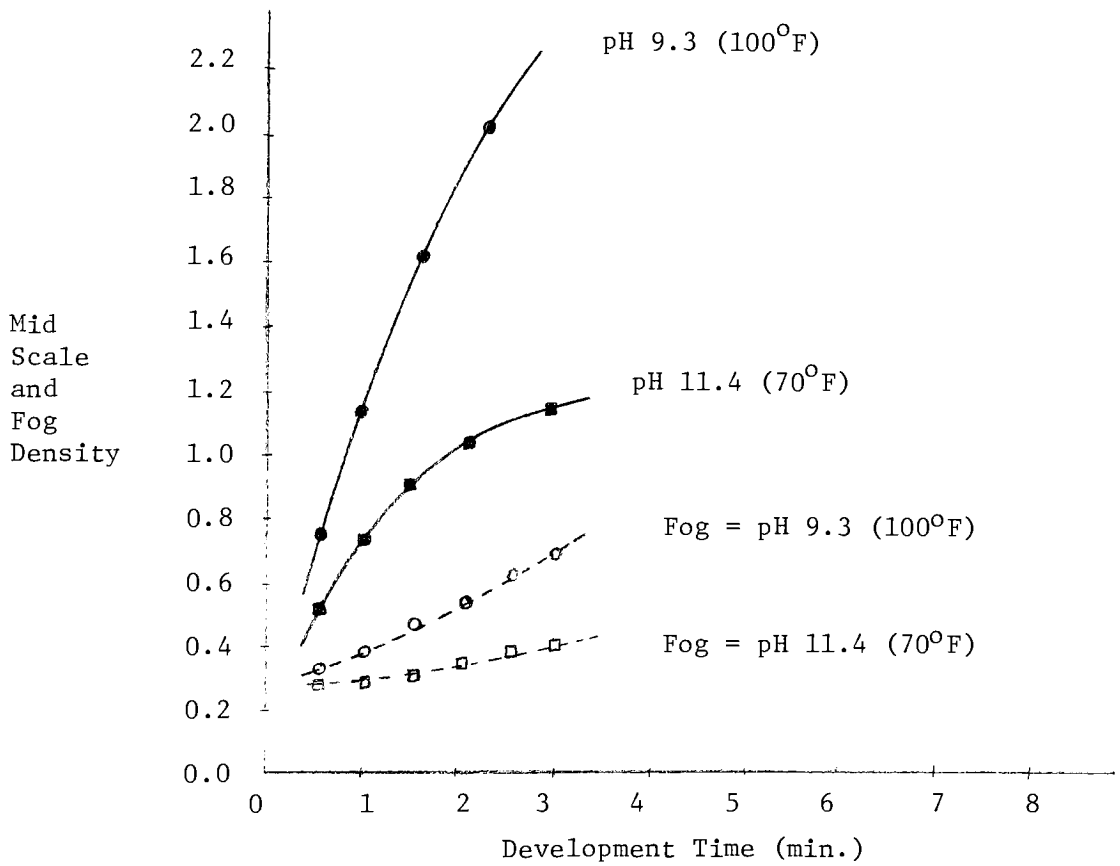

Figure 13 - Comparison of Development and Fog Rates at High Temperature (100°F) and High pH (11.4).

However, the edge effect increase was greater in the latter case. The reasons for this apparent anomaly are two-fold. The first is that the fog levels are much higher at high temperatures, as shown in Figure 13. This reduces the inhibitor concentration gradient across the edge, decreasing the adjacency effect. The second factor involved is an apparent increase in the diffusion of bromide ion at higher temperatures. This is evident from an increase in the width of the edge effect at high temperatures, and is illustrated in Figure 14. This would reduce the bromide ion effect, since it is able to diffuse out of the film more rapidly.

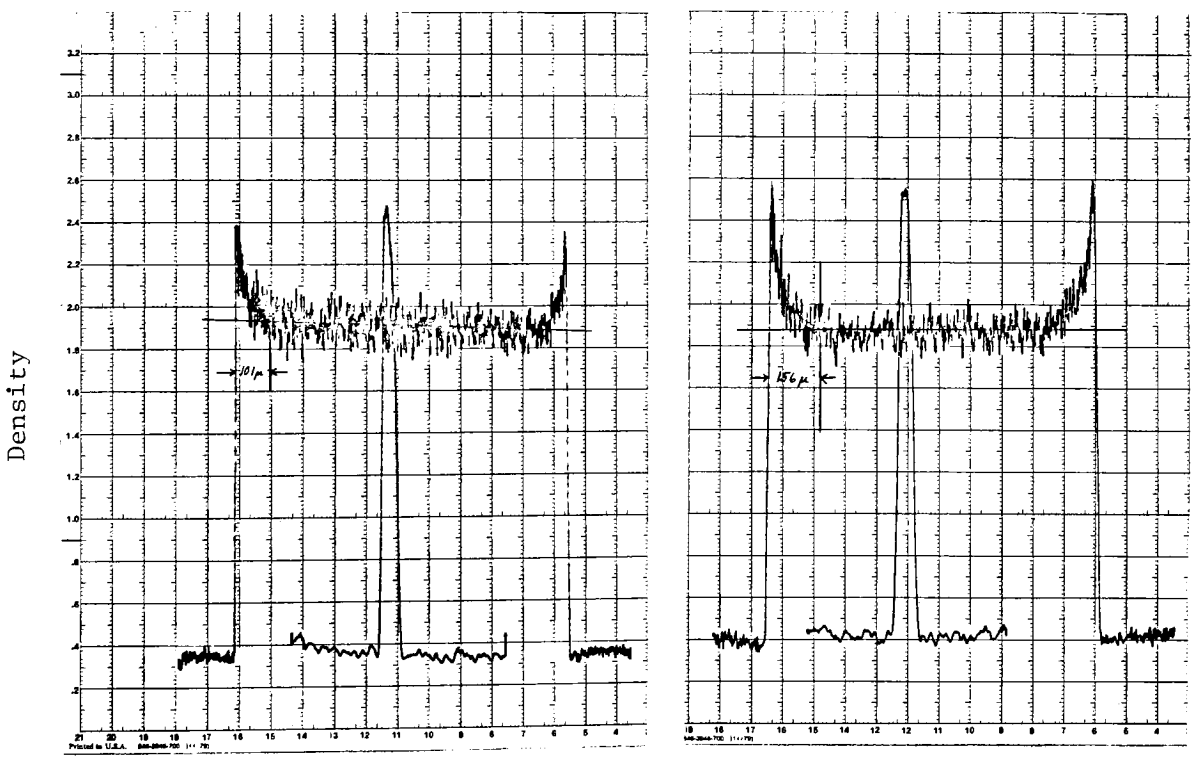

D-76 (70°F)
Dev. Time = 6 min.

PZ-13 (100°F)
Dev. Time = 1 1/2 min.

Figure 14 - Effect of Developer Temperature on Edge Width Using Microdensitometer Traces of X-ray Lines.

2(b) Metol at 0.2 g/l

Similar experiments were conducted at the very low Metol level (0.2 g/l). Since the adjacency effects produced under these conditions are much more pronounced than those obtained at higher Metol levels, these variations yielded different results than those previously observed.

The effect of adding sodium sulfite to a low-Metol developer is shown in Figure 15.

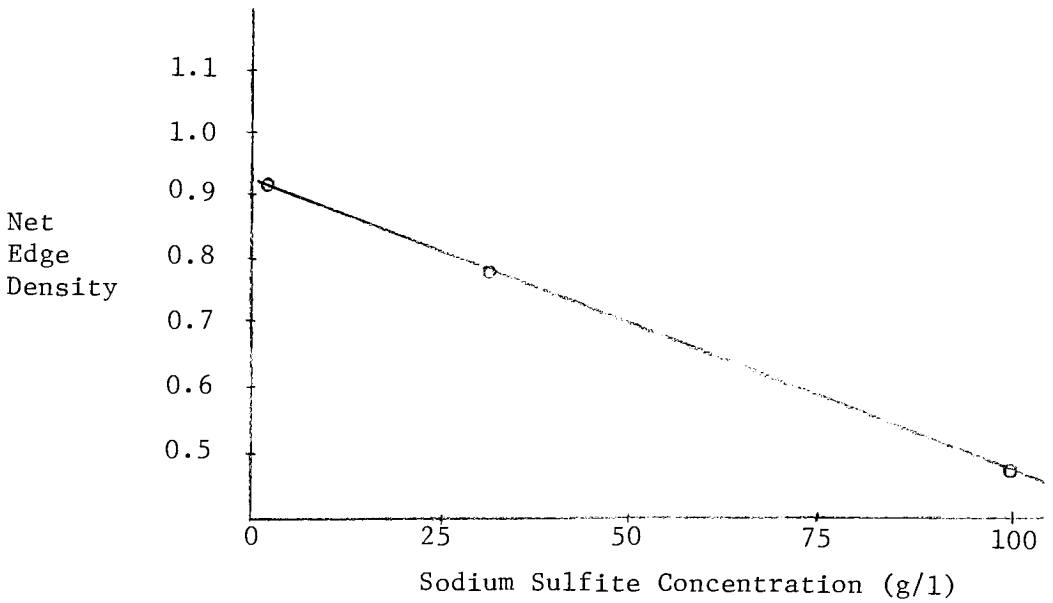

Figure 15 - Net Edge Density as a Function of Sulfite Level at 0.2 g/l of Metol.

It can be seen that the edge effect was substantially reduced as the sulfite level is increased. This is likely due to the silver halide solvent action of sodium sulfite.[48]

This solvent action results in less silver development everywhere reducing the amount of edge enhancement possible. This is demonstrated in Figure 16 using the uninhibited development rates given by the 10μ X-ray line data.

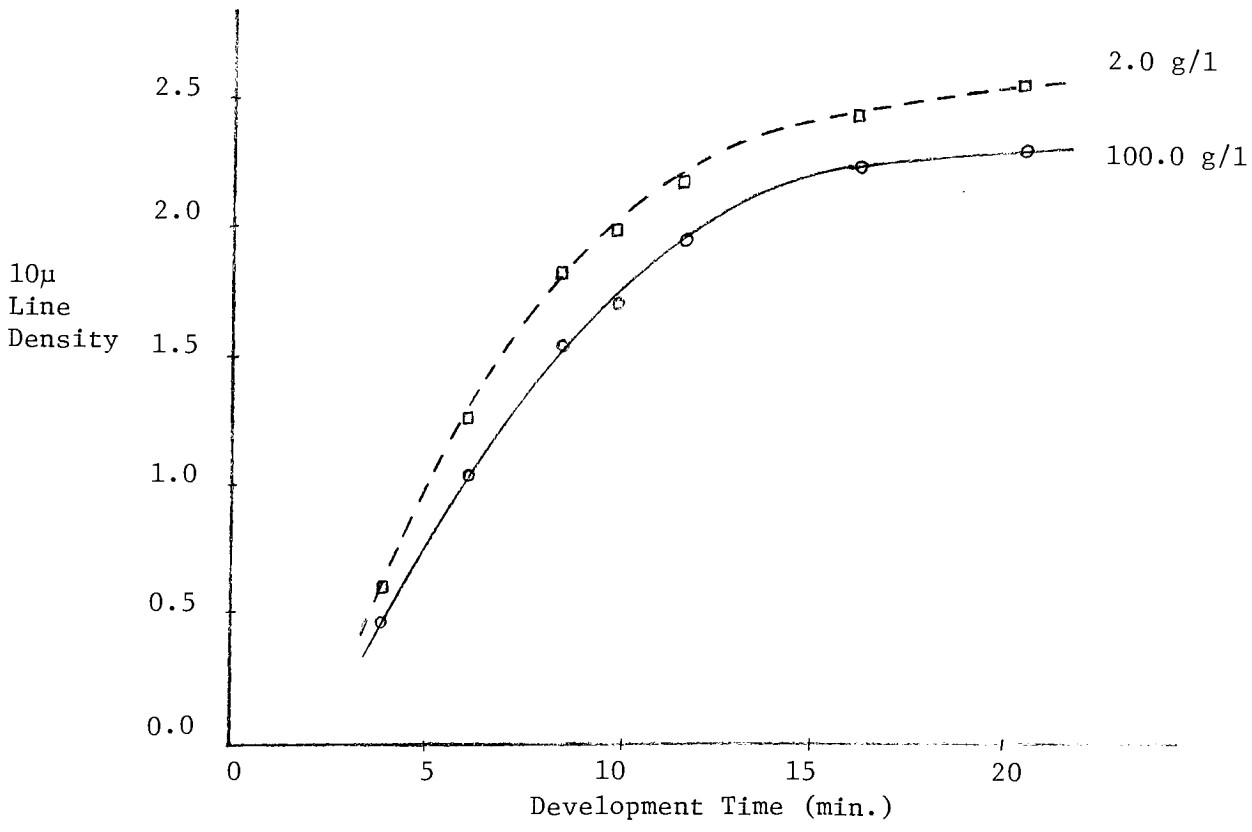

Figure 16 - Effect of Sulfite Level on the Uninhibited Density with Metol at 0.2 g/l

Since the uninhibited density represents the degree of enhancement theoretically possible, it is evident from these data that lower adjacency effects should result at higher sulfite levels, as shown in Figure 17.

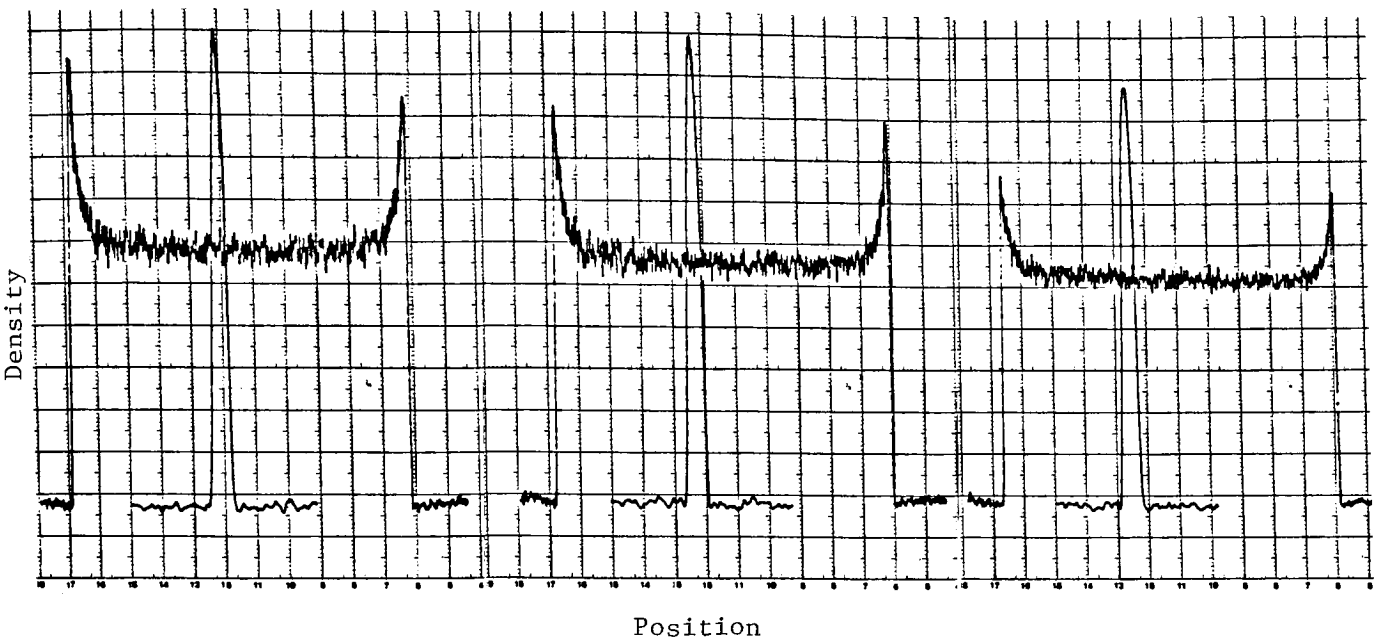

PZ-71	PZ-75	PZ-76
2.0 g/l Sulfite	30.0 g/l Sulfite	100.0 g/l Sulfite

Figure 17 - Effect of Sulfite Level on Adjacency Effects at 0.2 g/l of Metol Using Microdensitometer Traces of X-ray Lines.

The addition of hydroquinone to a low-Metol developer also resulted in substantially reduced edge effects. This is not surprising, since the high adjacency effects obtained in the absence of hydroquinone are due to developing agent exhaustion. When hydroquinone is introduced to the developer, oxidized Metol is regenerated.[49] This effectively increases the Metol concentration as well as the development rate, preventing Metol from becoming exhausted. Since the exhaustion mechanism responsible for the high adjacency effects is ruined, the edge effect is decreased. These results are clearly evident from the net edge density plot given in Figure 18 and the development rate curves shown in Figure 19.

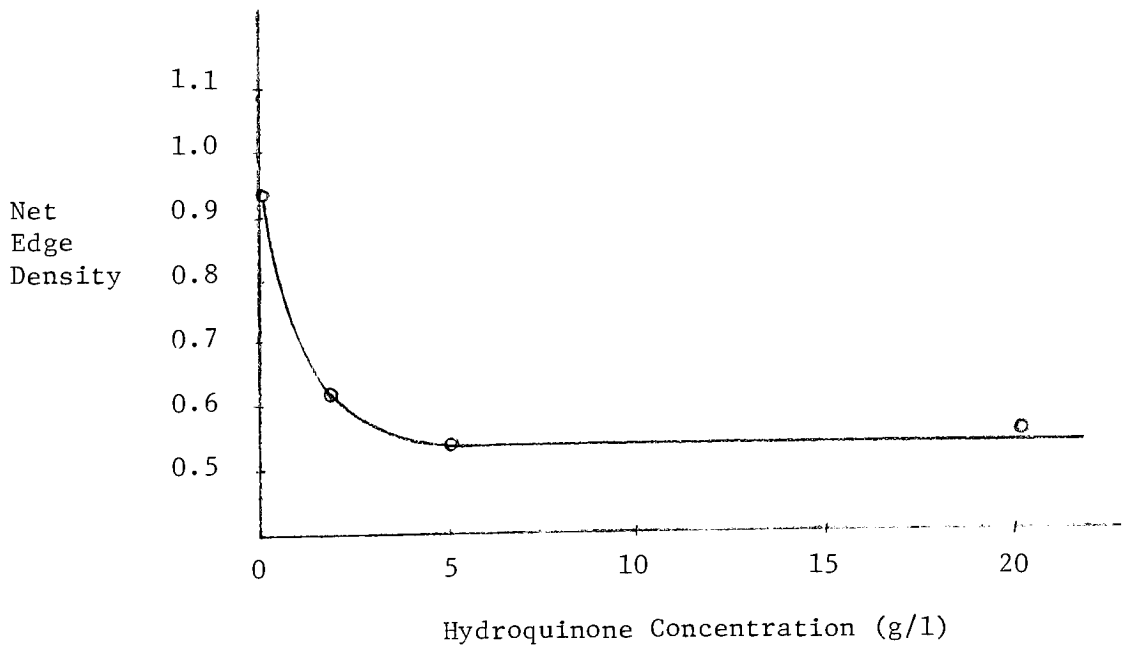

Figure 18 - Net Edge Density as a Function of Hydroquinone Concentration at 0.2 g/l of Metol.

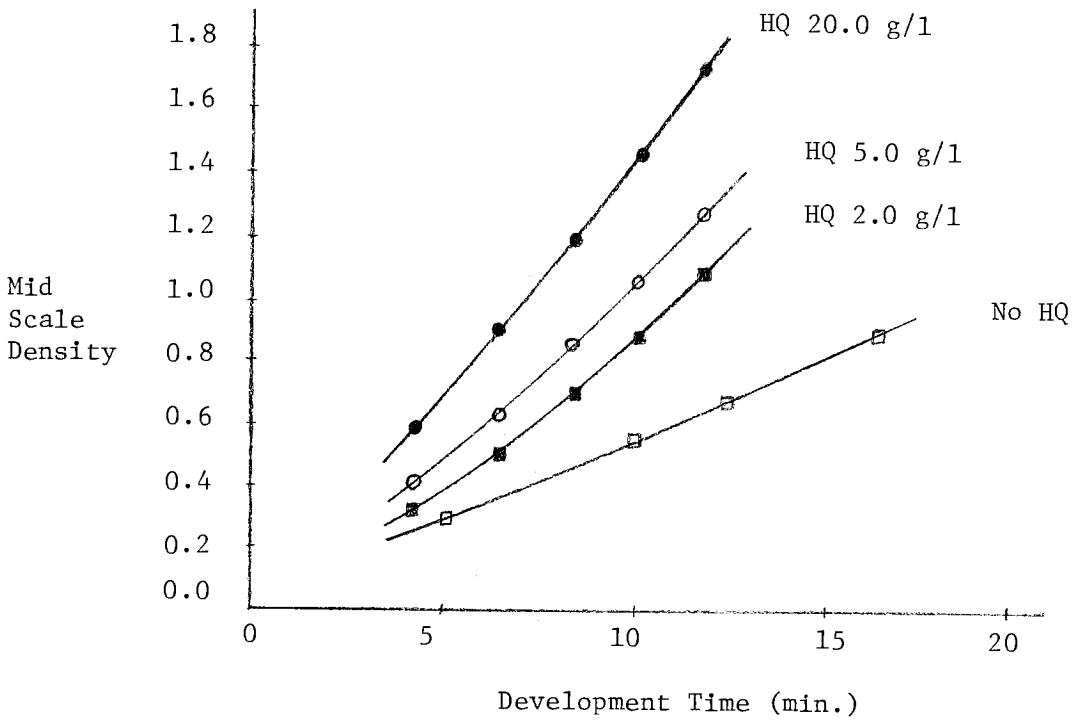

Figure 19 - Effect of Hydroquinone on the Development Rate of Low-Metol (0.2 g/1) Developers.

The effect of pH on adjacency effects produced by low-Metol developers was also investigated. The results of this study are depicted in Figure 20.

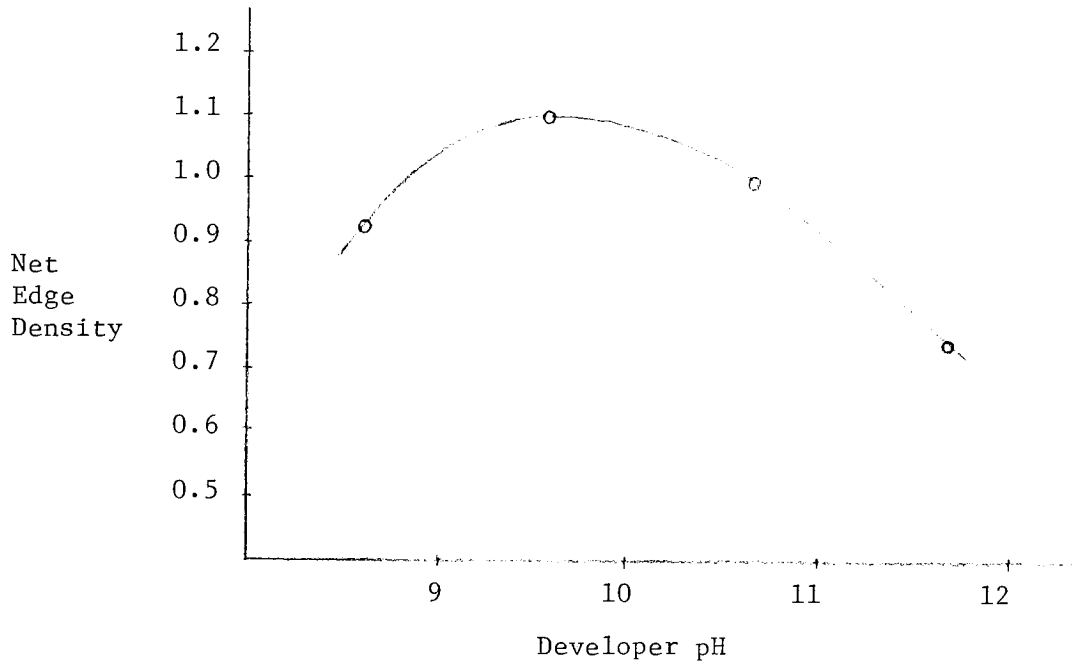

Figure 20 - Net Edge Density as a Function of pH at 0.2 g/l of Metol.

From this plot, it can be seen that edge effects increase with pH up to an optimum value of approximately 9.6, then decrease at higher pH values. Hence, a moderate boost in pH allows developing agent exhaustion to occur more rapidly, favoring the formation of high adjacency effects. As the pH is raised beyond the optimum value, the increase in fog becomes significant. More active developer is used up in the unexposed areas making it unavailable for enhancing density at the edge. Generally, edge effects fall off at high

fog levels. The edge effects produced with PZ-62 (pH 9.6) are the highest adjacency effects obtained under the conditions of these experiments. Examples of these effects at various pH values are illustrated in Figure 21.

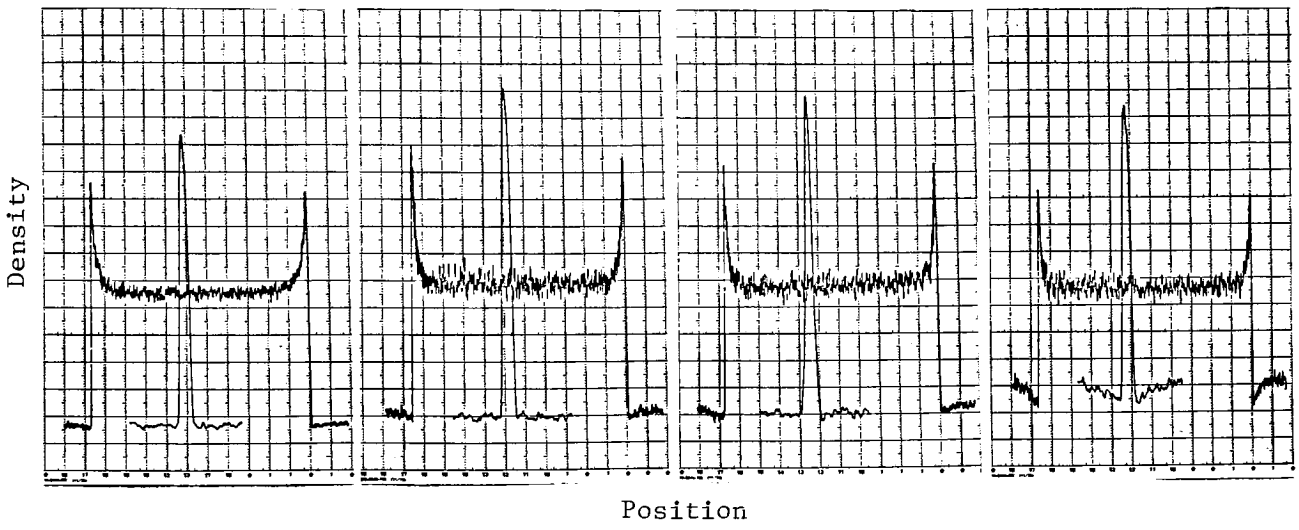

PZ-61	PZ-62	PZ-63	PZ-64
(pH 8.6)	(pH 9.6)	(pH 10.6)	(pH 11.6)

Figure 21 - Effect of pH on Adjacency Effects with Metol at 0.2 g/l Using Microdensitometer Traces of X-ray Lines.

A summary of adjacency effects produced by Metol development is shown in Figure 22.

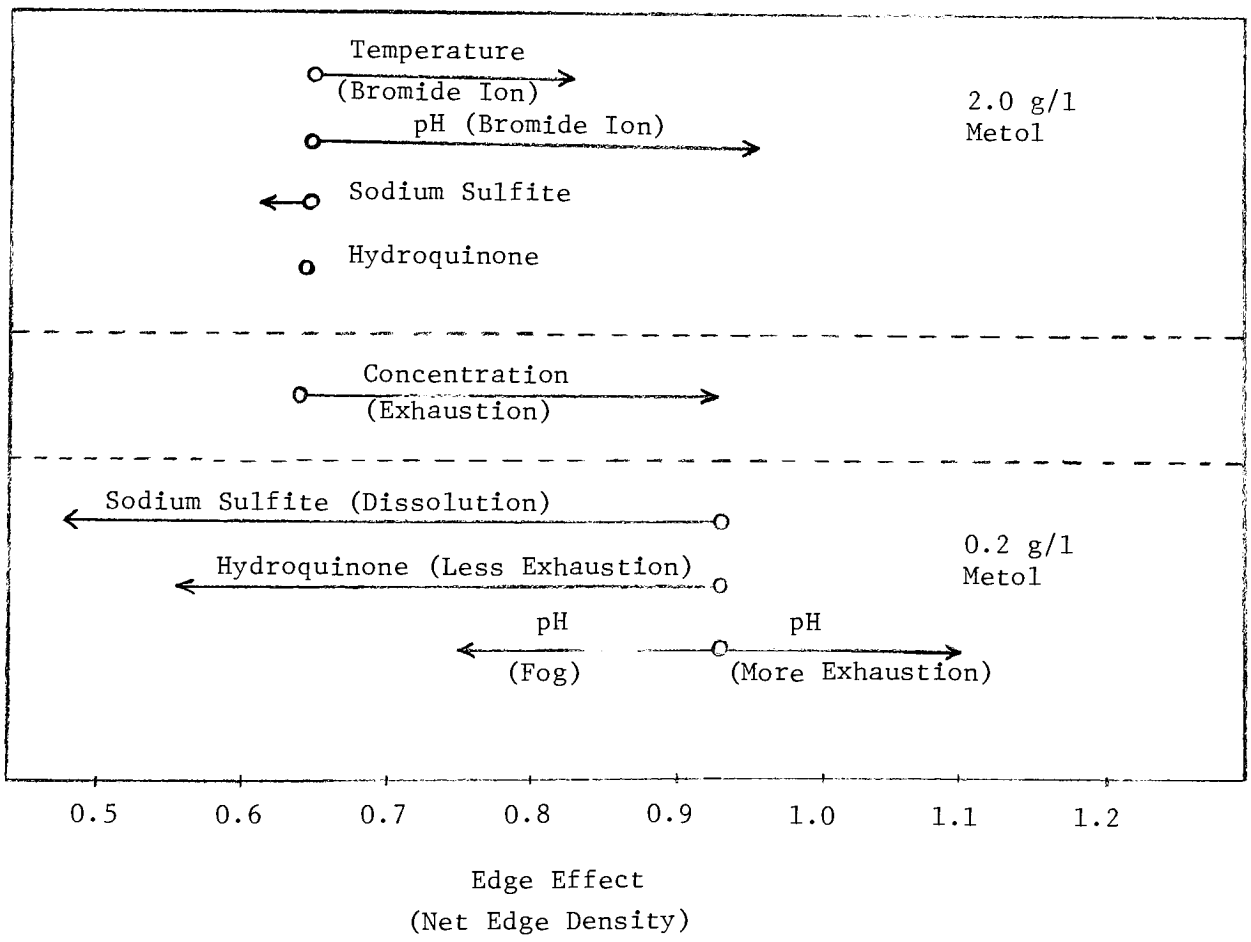

Figure 22 - Summary of Adjacency Effects Produced with Metol Development.

Right way effects occur when:

1) Metol concentration is reduced
2) pH is drastically increased at 2.0 g/l Metol
3) temperature is drastically increased at 2.0 g/l Metol
4) pH is moderately increased at 0.2 g/l Metol.

Wrong way effects occur when:

1) sulfite level is increased at 0.2 g/l Metol
2) hydroquinone is used at 0.2 g/l Metol
3) high fog levels are present.

3) Phenidone Developer Variations

Since high adjacency effects were also observed with the POTA formula, it was used as a starting point for studying developer variations with Phenidone. In general, adjacency effect behavior with Phenidone developers differ considerably from that observed with Metol developers.

Unlike Metol developers, Phenidone developers do not form high adjacency effects by exhausting the developing agent. This is likely due to the fact that development with Phenidone is much slower than with Metol under similar dilute conditions, as shown in Figure 23.

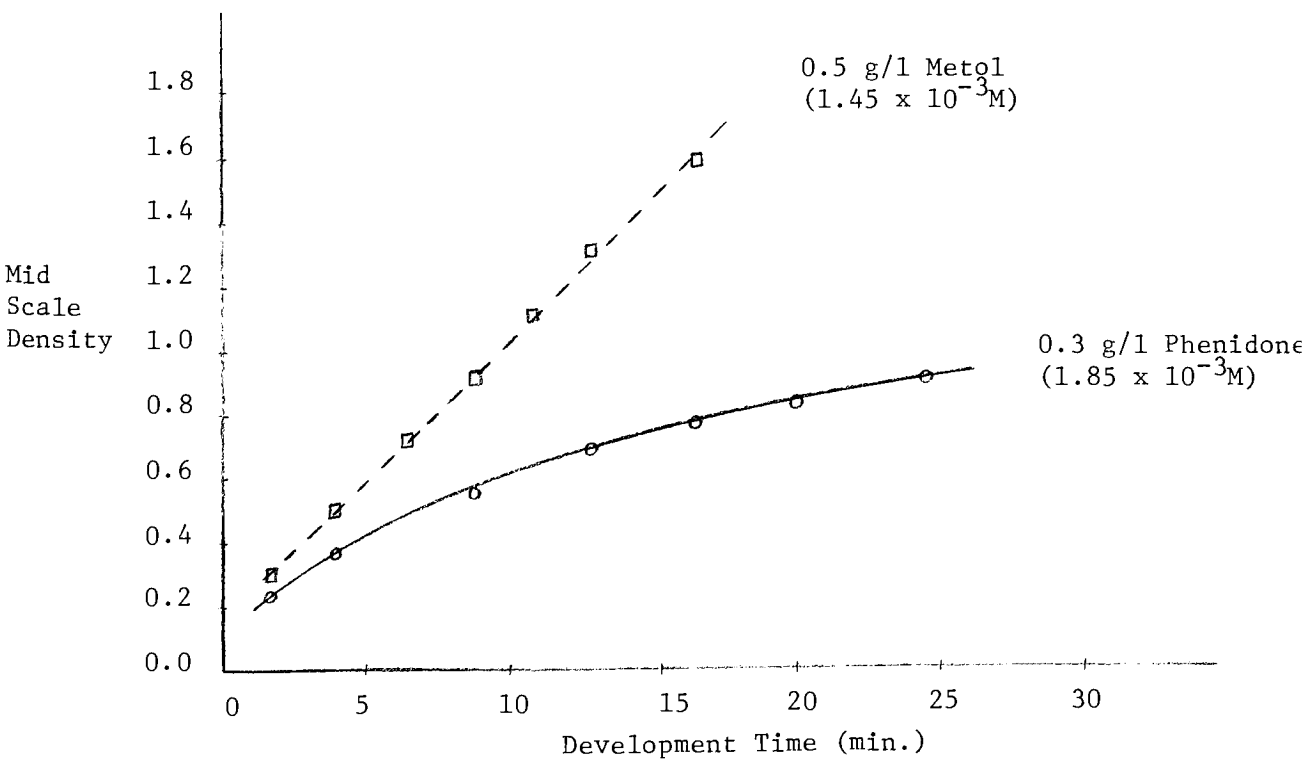

Figure 23 - Comparison of Development Rates with Dilute Metol and Phenidone Developers.

The effect of Phenidone concentration on edge effects is illustrated in Figure 24.

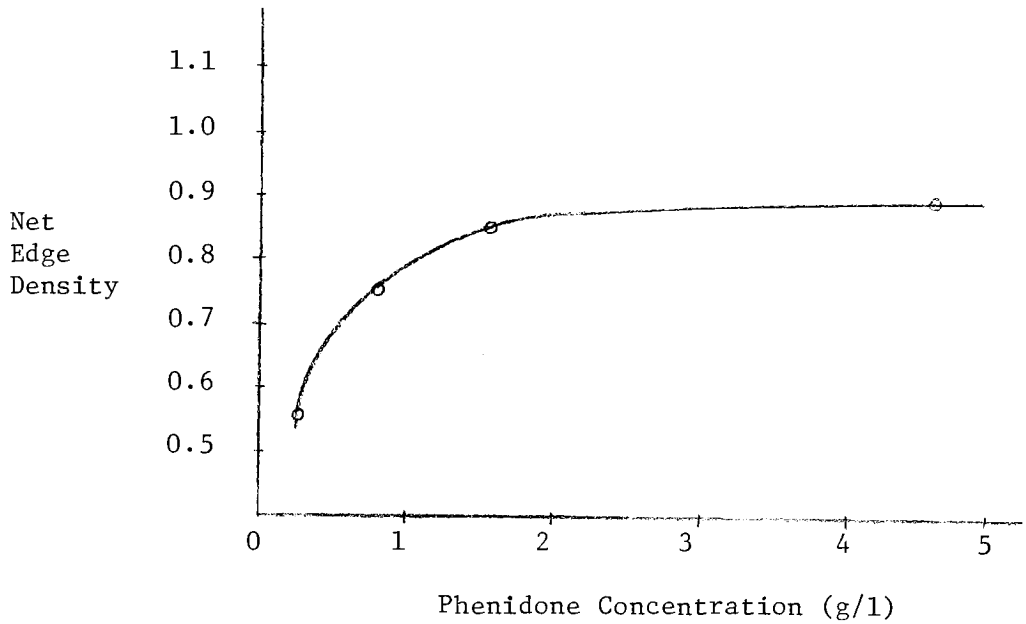

Figure 24 - Net Edge Density as a Function of Phenidone Concentration.

From these results, it is apparent that Phenidone developers behave quite differently than Metol developers as a function of developing agent concentration. At Phenidone levels below 1.0 g/l, adjacency effects decline substantially as the concentration decreases. This trend suggests that edge effects formed by Phenidone development occur via a different mechanism.

Development with Phenidone was also studied as a function of sodium sulfite level. These results are depicted in Figure 25.

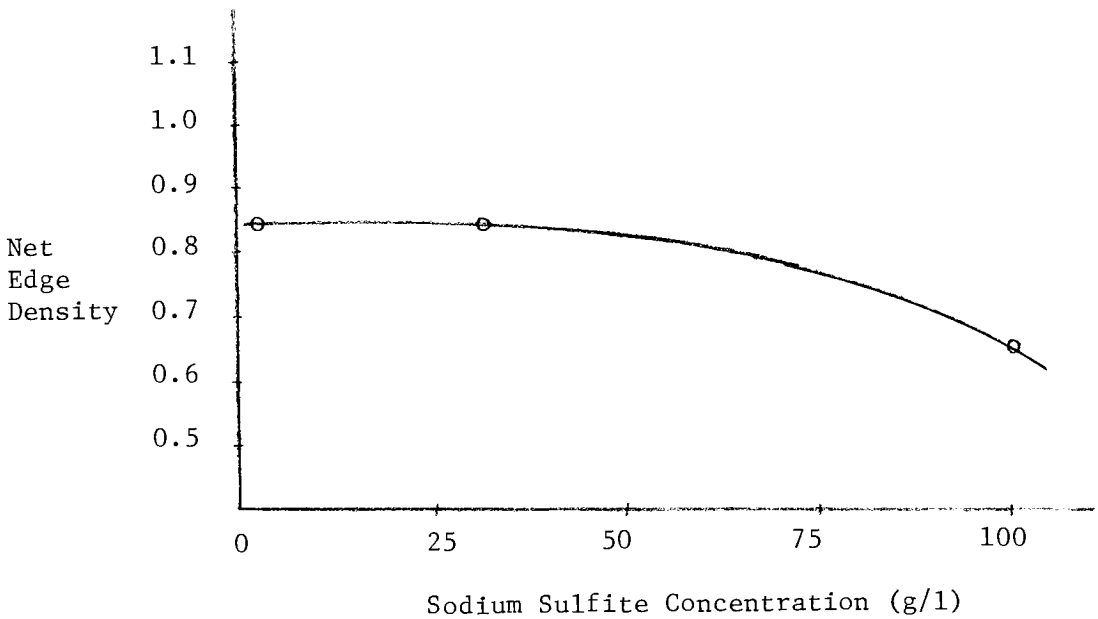

Figure 25 - Net Edge Density as a Function of Sulfite Level at 1.5 g/l of Phenidone.

No change is observed between 2.0 g/l and 30.0 g/l of sulfite, but a significant reduction of the edge effect occurs at the high sulfite level (100.0 g/l), as also seen with low-Metol developers. Presumably, it occurs for the same reason, namely, solvent action. This is once again supported by the uninhibited densities for each case, given by the 10μ X-ray line data. This is illustrated in Figure 26.

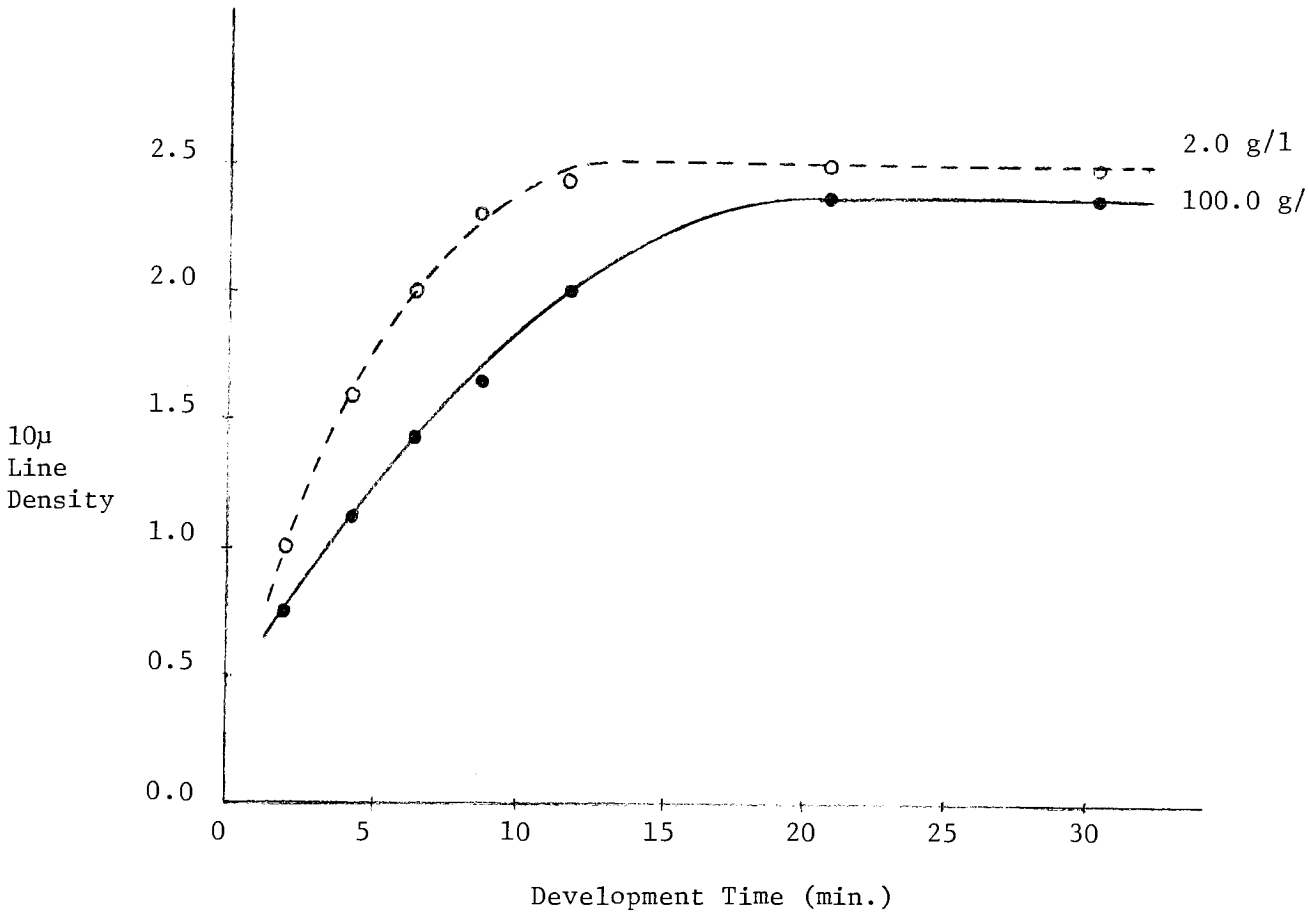

Figure 26 - Effect of Sulfite Level on the Uninhibited Density with Phenidone at 1.5 g/1.

Edge reduction at high sulfite levels is less severe with Phenidone, than with low-Metol development. This is likely due to the fact that Phenidone acts as a "total grain developer", while Metol is a "partial grain developer".[50] If a significant fraction of exposed silver halide grains

are completely developed shortly after development is initiated, sulfite will have little chance to etch those silver halide crystals. The converse is true when the individual grains develop slowly. Further implications of these development phenomena are discussed in the following section.

Adjacency effects produced by Phenidone development are also influenced by pH, as shown in Figure 27.

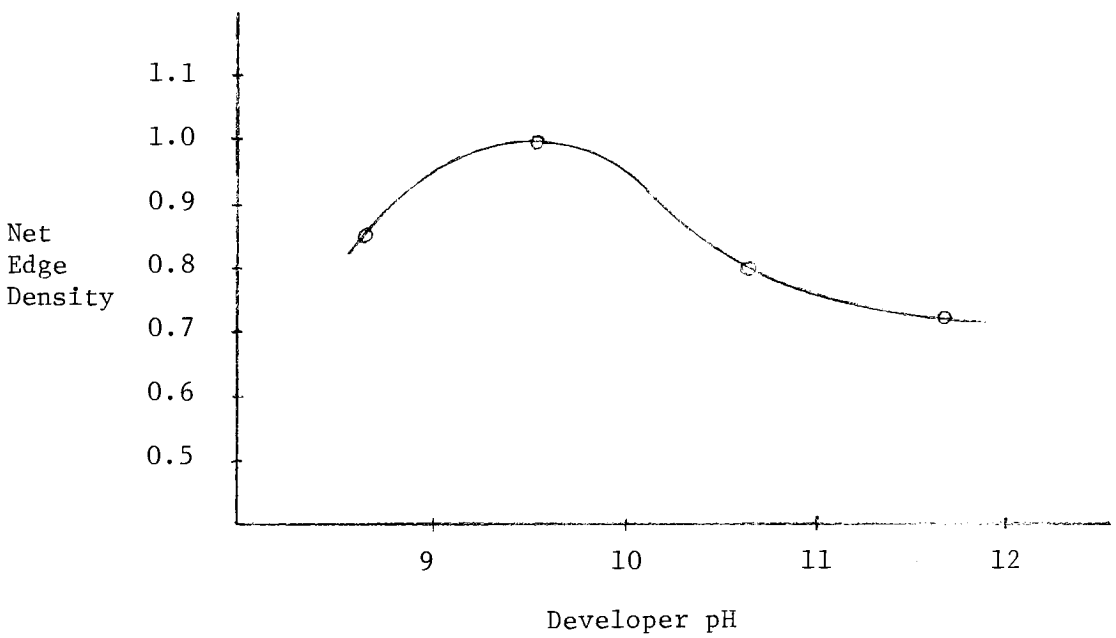

Figure 27 - Net Edge Density as a Function of pH at 1.5 g/l of Phenidone.

Edge effects are enhanced as the pH increases moderately, then decline at higher pH values. The optimum pH for edge enhancement is approximately 9.6. The reduced enhancement at higher pH values is again likely due to high fog levels, as stated previously.

Perhaps the most interesting behavior observed with Phenidone development occurred when hydroquinone was introduced to the developer. A dramatic reduction in edge enhancement was seen in the presence of hydroquinone, as illustrated in Figures 28 and 29.

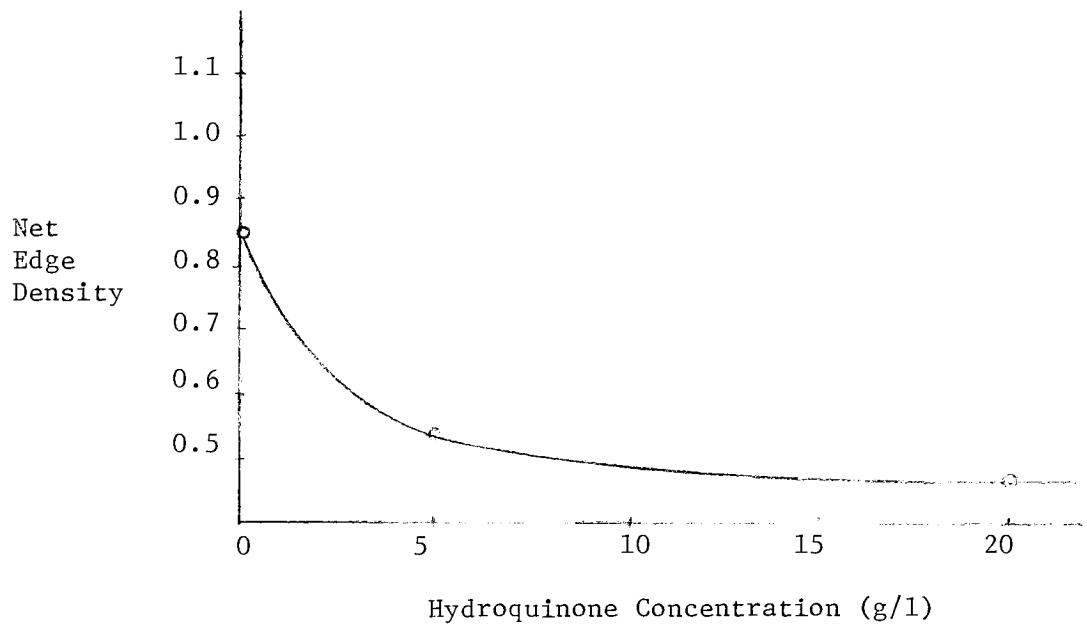

Figure 28 - Net Edge Density as a Function of Hydroquinone Concentration at 1.5 g/l of Phenidone.

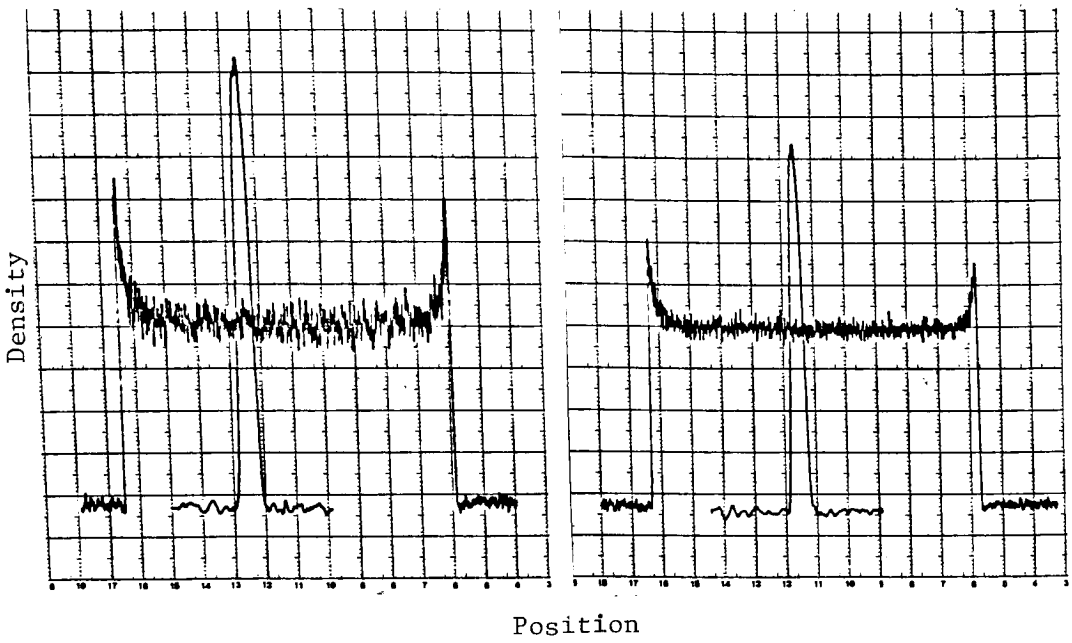

POTA	PZ-143
Phenidone 1.5 g/l	Phenidone 0.3 g/l Hydroquinone 5.0 g/l

Figure 29 - Effect of Hydroquinone on Adjacency Effects with Phenidone Development Using Microdensitometer Traces of X-ray Lines.

This is similar to the response observed when hydroquinone was added to the low-Metol developer (see Figure 18). With low-Metol developers, hydroquinone accelerates the rate of development by regenerating Metol. This destroys the exhaustion mechanism responsible for edge enhancement in the absence of hydroquinone. However, it is apparent from the data given in Figure 24 that exhaustion of the developing agent does not occur with Phenidone development. This implies that hydroquinone is serving a different function in this case.

The results depicted in Figure 29 also show that when hydroquinone was added to a Phenidone developer, the granularity decreased. The microdensitometer traces display a reduction in edge density and considerably less density fluctuation (granularity) across the macro area with PZ-143 versus POTA. A certain amount of decreased granularity was expected just due to the reduced edge effect. However, it appears that the number of developed centers was increased by the addition of hydroquinone. This is illustrated in Figure 30 using photomicrographs of the developed grains for areas of the processed films which have matched exposure and density.

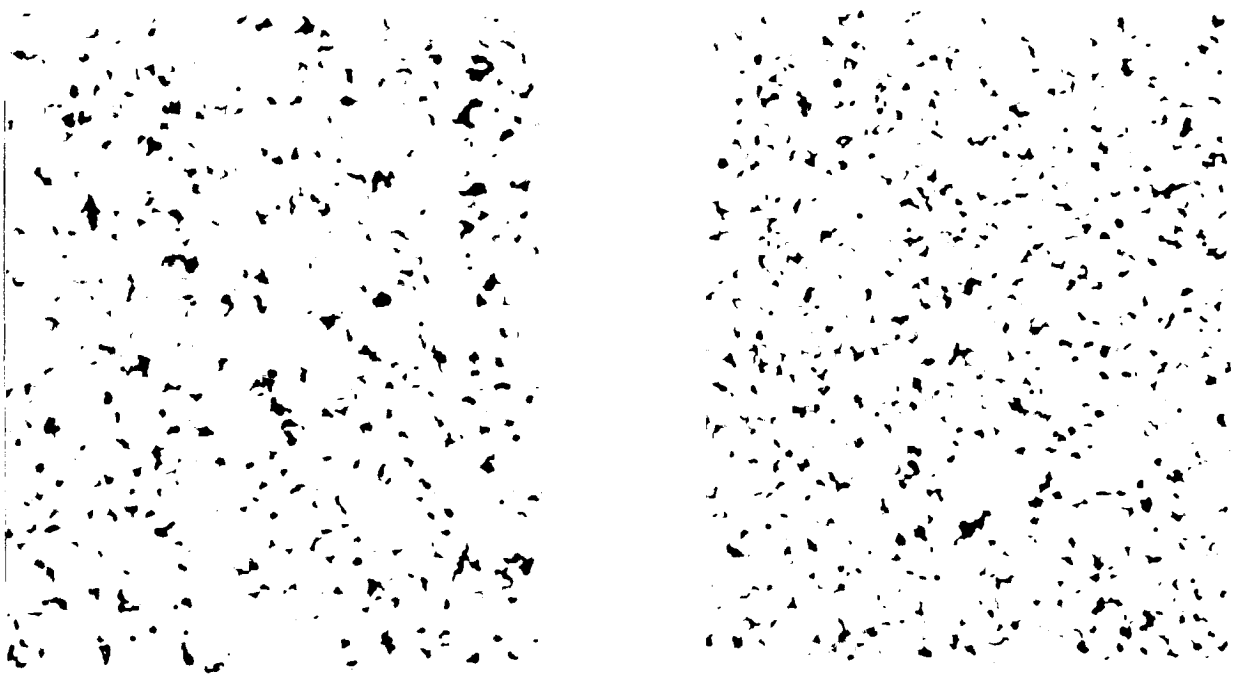

POTA Mag. = 1500X PZ-143

Figure 30 - Photomicrographs of developed Tri-X grains for POTA and PZ-143 at matched exposure and density (D_v = 0.34)

The photomicrographs show fewer grains more completely developed with POTA, while the PZ-143 developer seems to develop more grains in a given area, but to a lesser extent.

These results might be explained if we suppose that the addition of hydroquinone results in a shorter development induction period for each individual, exposed grain.[51] In this case, each exposed grain will start developing sooner than it would in the absence of hydroquinone.[52] Since more grains are developing in a given time frame, less development of each individual grain will be necessary to achieve a certain density.[53] The net result in this situation is more developed silver centers, hence, lower granularity.

Since hydroquinone is very inactive as a developing agent at pH 8.6, it likely reacts with an oxidized form of Phenidone to regenerate Phenidone (active developing agent).[54] This not only increases the effective concentration of active developing agent, but also removes development inhibiting oxidized Phenidone.[55] Since the rate of development with 0.3 g/l (1.85×10^{-3}M) of Phenidone and 2.0 g/l (18.16×10^{-3}M) of hydroquinone (20.01×10^{-3}M total) is much faster than with 4.5 g/l (27.75×10^{-3}M total) of Phenidone, it seems plausible that hydroquinone also serves to remove development inhibiting products, instead of merely increasing the concentration of active developing agent. These results are given in Figure 31.

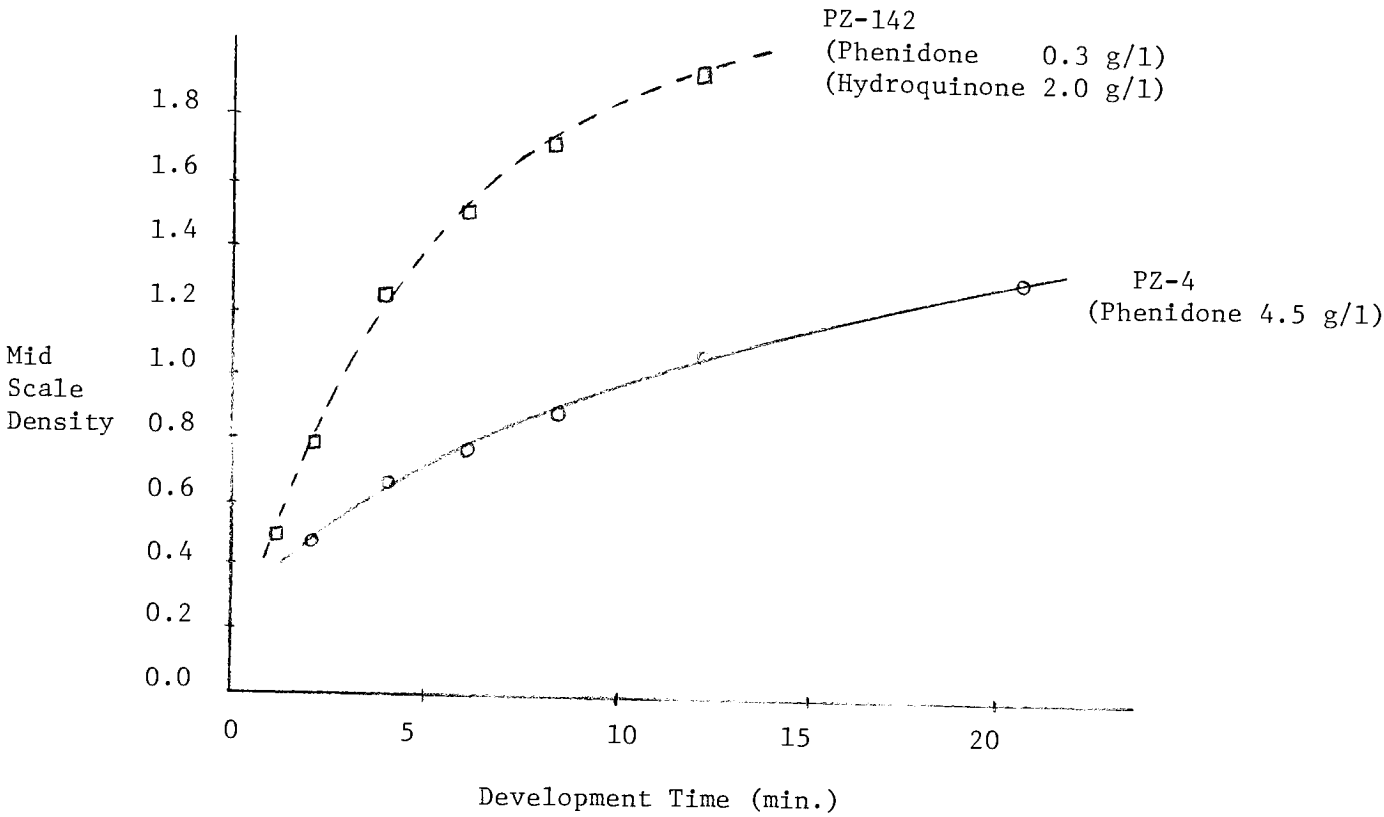

Figure 31 - Effect of Hydroquinone on the Development Rate with Phenidone.

While PZ-142 has a much faster macro area development rate, it has only a slightly faster uninhibited development rate, as shown in Figure 32.

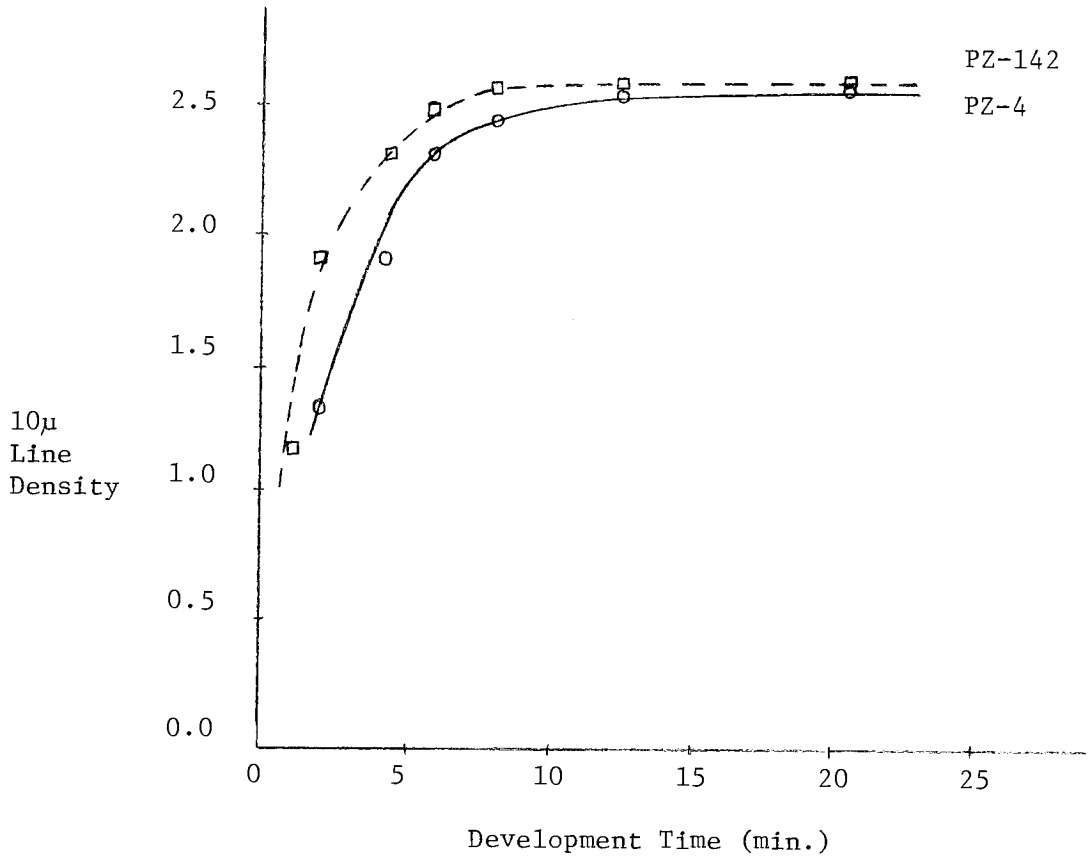

Figure 32 - Effect of Hydroquinone on the Uninhibited Development Rate with Phenidone.

This demonstrates that the slow development rate of PZ-4 is largely due to development inhibition. This argument is also consistent with previous observations which illustrated high adjacency effects at high Phenidone concentrations as opposed to lower adjacency effects with the combination of Phenidone and hydroquinone. Hence, it appears that oxidized Phenidone acts as a development inhibitor, while hydroquinone acts as an oxidized Phenidone acceptor. This conclusion explains why Phenidone developers exhibit high adjacency effects over a wide range of development conditions, while Metol developers do not.

A summary of adjacency effects produced by Phenidone development is shown in Figure 33.

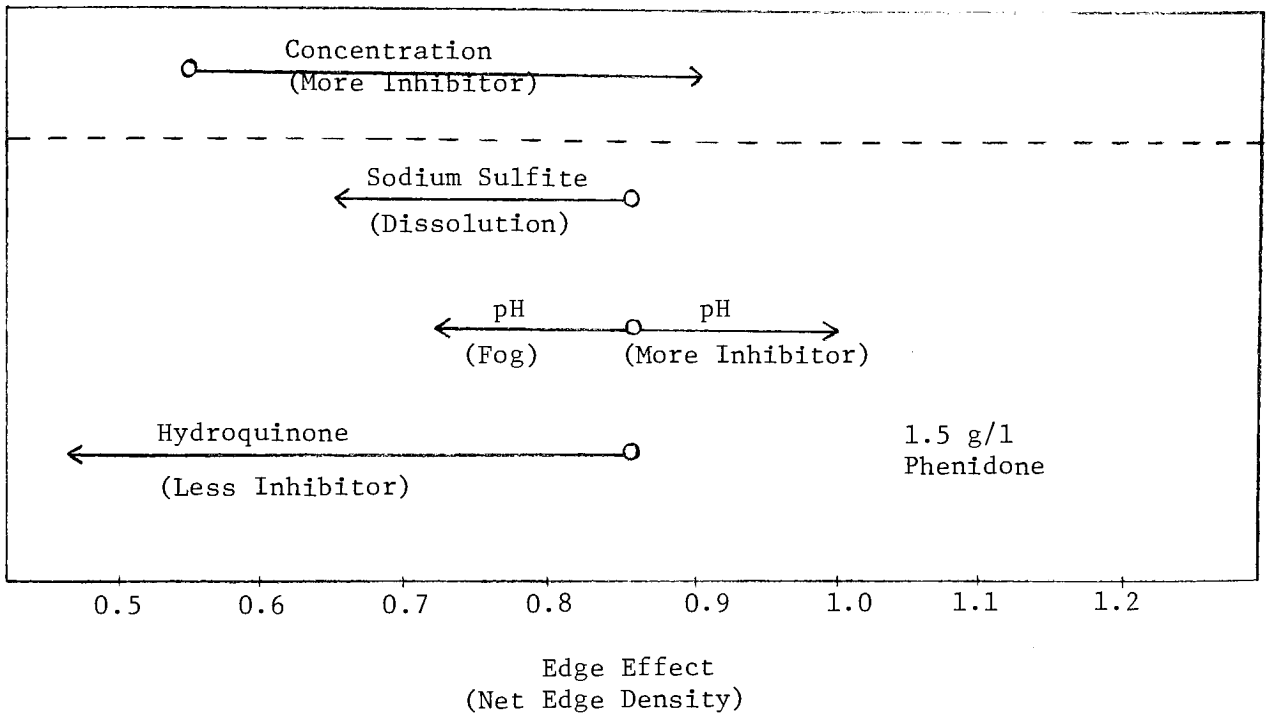

Figure 33 - Summary of Adjacency Effects Produced with Phenidone Development.

Right way effects occur when:

1) Phenidone concentration is increased

2) pH is moderately increased with 1.5 g/l Phenidone.

Wrong way effects occur when:

1) Sulfite level is increased with 1.5 g/l Phenidone
2) hydroquinone is used with 1.5 g/l Phenidone
3) high fog levels are present.

4) Acutance - Granularity Relationship

It was apparent from the results obtained from these studies that improved edge enhancement during development was accompanied by increased granularity. Hence, experiments were designed to explore the nature of this trade-off and relate these results to the image seen in photographic prints.

The following films and developers were used in this investigation:

Films	Developers
KODAK Panatomic-X	D-76
KODAK Plus-X	PZ-143
KODAK Tri-X	PZ-21
	POTA

D-76 was used as the control developer. PZ-21 and POTA are "high-acutance" developers employing Metol and Phenidone as developing agents, respectively. PZ-143 represents an intermediate postion between D-76 and the "high-acutance" developers.

The films were processed to approximately matched contrast indices. An aim value of 0.60 was used. Slight differences in speed (± 1/2 stop from D-76) were obtained among the developers. D-log E curves, X-ray lines, RMS granularity measurements, MTF curves with corresponding CMT values, and definition pictures were obtained for each film-developer combination as described in the experimental procedure.

4(a) Objective Evaluation

The values of speed, fog, contrast, index, CMT, and gamma-normalized RMS granularity are given in Table II.

Table II

Photographic Data for Various Film-Developer Combinations

Film	Developer	Dev. Time	Speed	Fog	C.I.	CMT	$\sigma_D/\gamma \times 10^3$
	D-76	4 min	214	0.26	0.65	92.5	10
KODAK	PZ-143	2 3/4 min	222	0.27	0.60	94.5	14
Pan-X	PZ-21	18 min	203	0.28	0.65	94.7	13
	POTA	17 min	230	0.33	0.65	95.9	20
	D-76	5 min	263	0.28	0.65	92.4	16
KODAK	PZ-143	3 3/4 min	259	0.34	0.63	93.5	22
Plus-X	PZ-21	20 min	245	0.36	0.61	95.2	24
	POTA	28 min	273	0.38	0.60	94.7	29
	D-76	5 1/2 min	312	0.32	0.58	90.9	21
KODAK	PZ-143	4 1/2 min	320	0.35	0.60	93.5	26
Tri-X	PZ-21	30 min	304	0.35	0.60	95.7	31
	POTA	30 min	322	0.40	0.61	94.3	37

The CMT values and granularity measurements are tabulated for equivalent exposures which yielded a mid-scale density. Corresponding microdensitometer traces of X-ray lines at roughly matched densities for the various film-developer combinations are given in Figure 34.

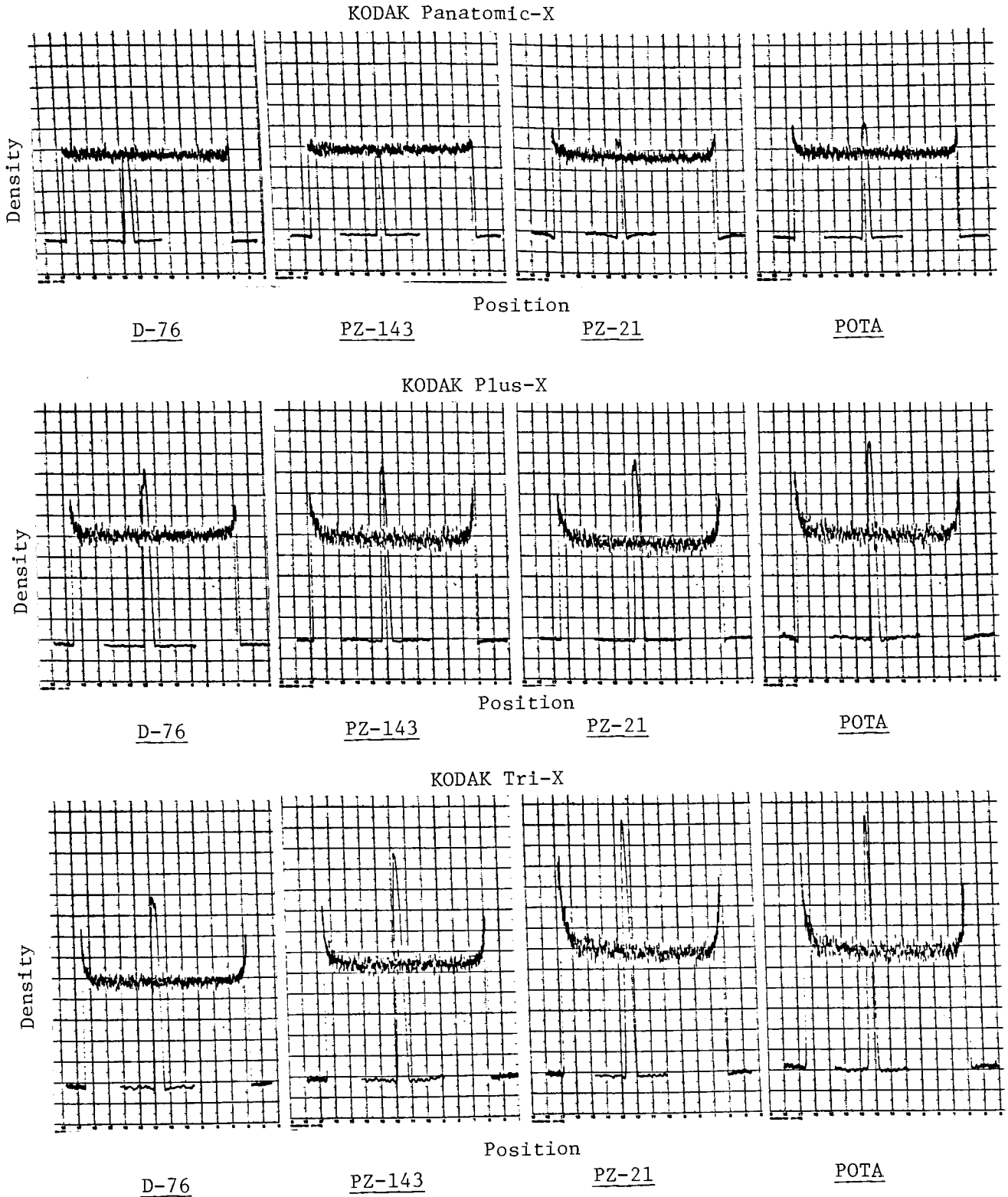

Figure 34 - Microdensitometer Traces of X-ray Lines for Various Film-Developer Combinations.

The MTF curves for the various developers with Panatomic-X, Plus-X, and Tri-X are given in Figures 35, 36, and 37, respectively.

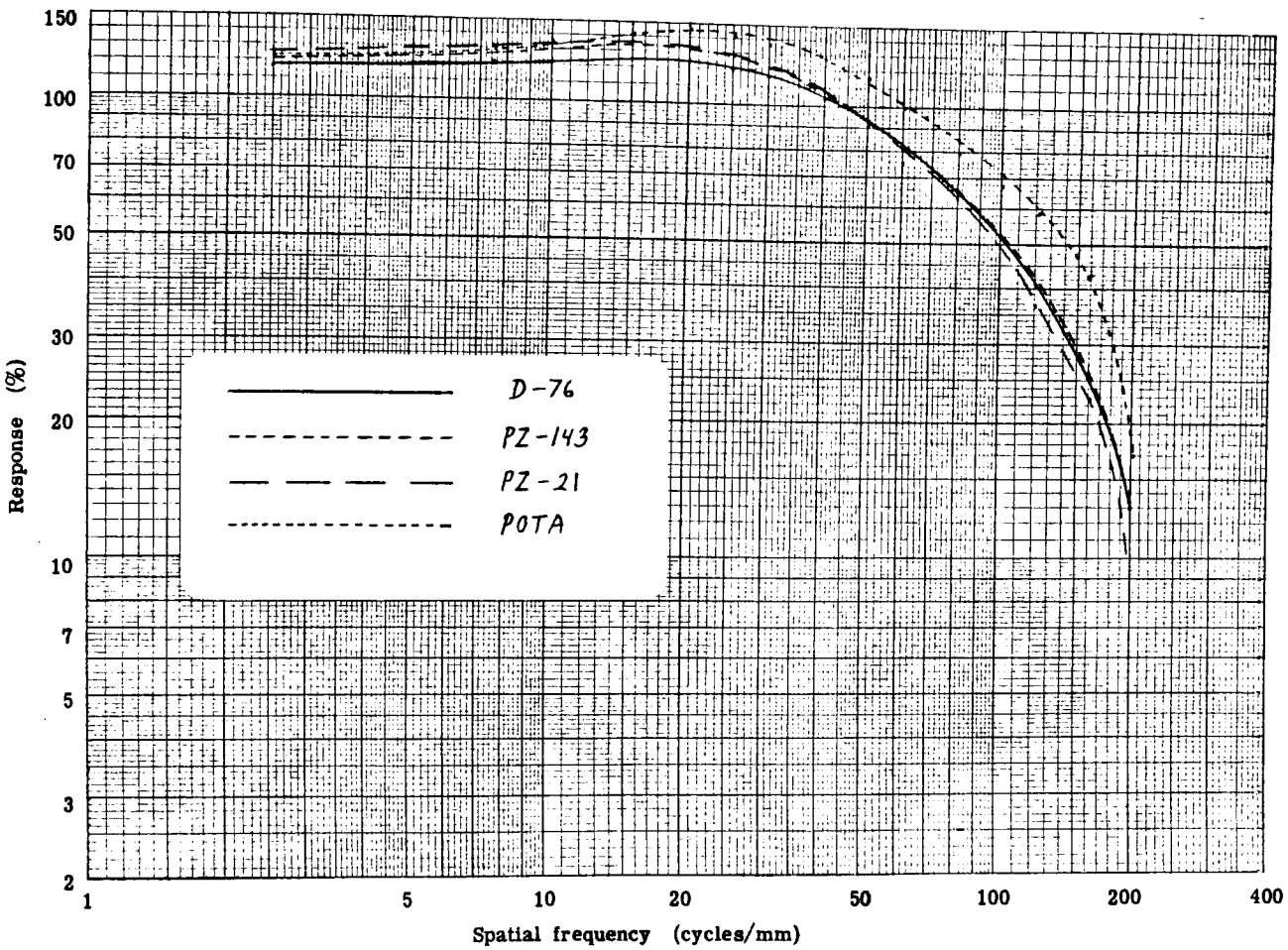

Figure 35 - MTF curves for D-76, PZ-143, PZ-21, and POTA with KODAK Panatomic-X Film.

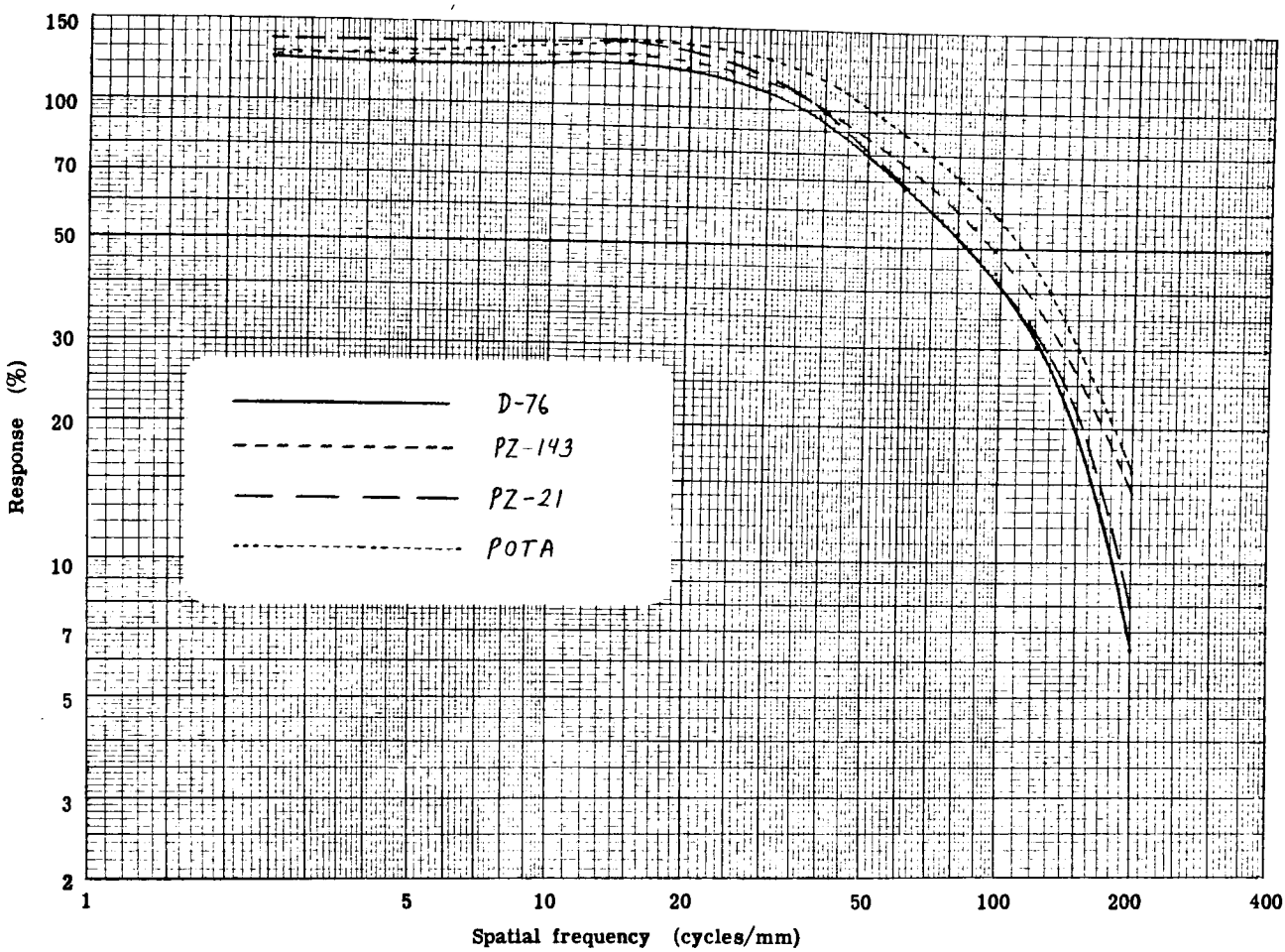

Figure 36 - MTF curves for D-76, PZ-143, PZ-21, and POTA with KODAK Plus-X Film.

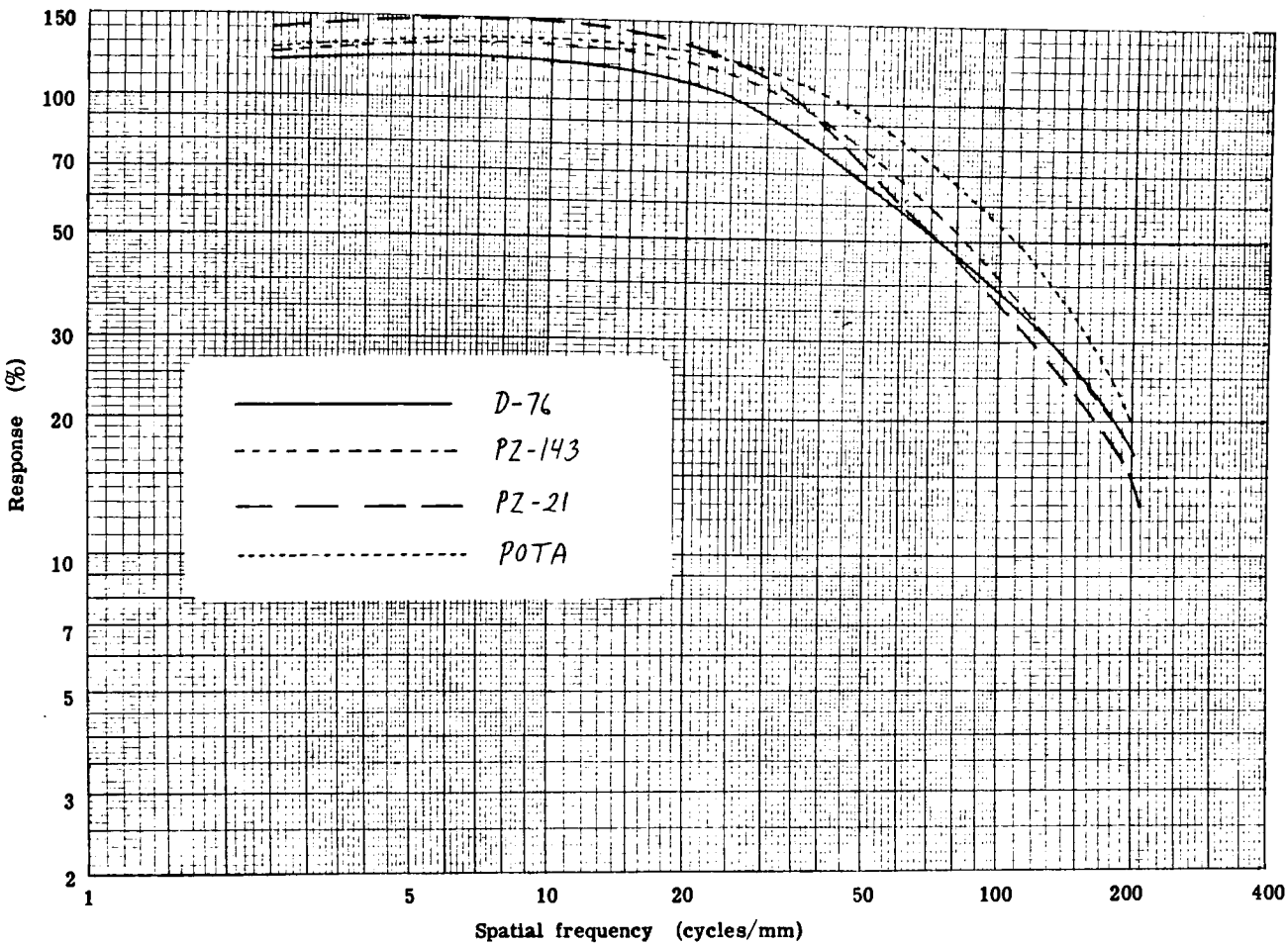

Figure 37 - MTF curves for D-76, PZ-143, PZ-21, and POTA with KODAK Tri-X Film.

Generally, PZ-143 yielded slightly higher acutance than D-76, while PZ-21 and POTA produced a greater acutance boost with each film. All three developers provided low-frequency (less than 50 cycles/mm) enhancement superior to that obtained with D-76. However, POTA yielded considerably greater high-frequency (greater than 50 cycles/mm) enhancement than the other developers. This is discussed in greater detail in the following section.

Definition pictures made at 12X enlargement from negatives of these film-developer combinations are included in Figures 47-58 at the end of this text.

The acutance-granularity trade-off obtained with these developers for each film is summarized in Figure 38.

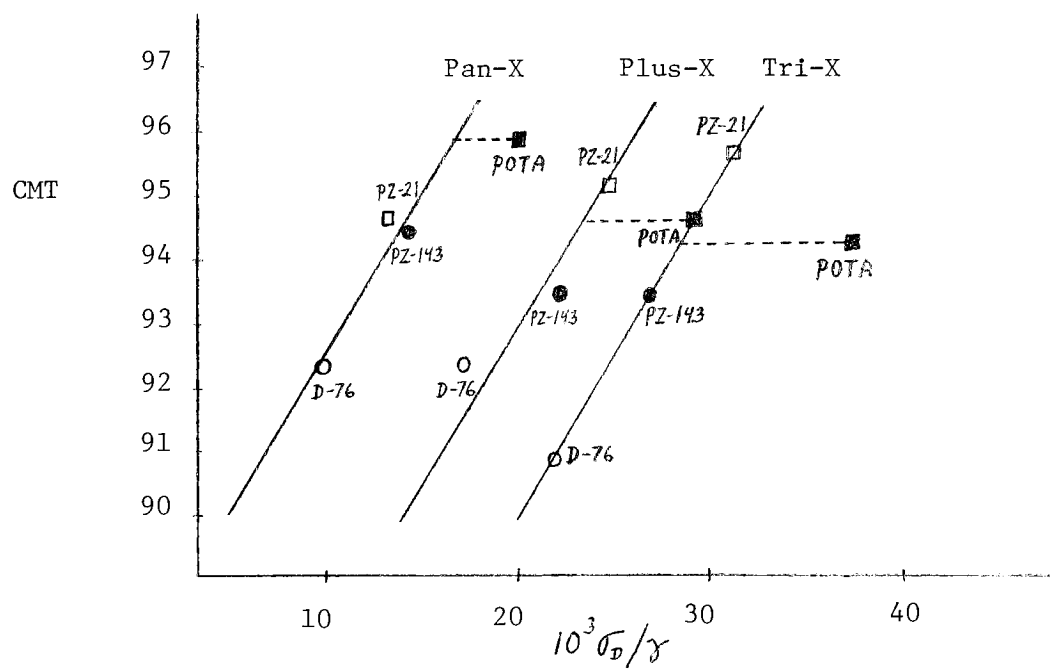

Figure 38 - CMT Acutance versus Gamma-Normalized RMS Granularity for the Various Film-Developer Combinations.

In general, as the acutance improves the granularity increases. The trade-off is approximately linear for each film except when POTA is used. The slope of the acutance-granularity lines are roughly equal for each film type. An acutance gain of 1 CMT unit results in an increase of 2 units of $10^3\sigma_D/\gamma$. The trade-off is obviously much less favorable with POTA development and becomes even more unfavorable as the film speed increases. These results indicate that the increase in granularity with POTA is much greater than deserved from normal acutance-granularity considerations.

Silver analyses of these film-developer combinations were obtained by X-ray fluorescence. The results show that considerably more silver is developed with POTA to achieve a given density with all three films. These data are given in Table III.

Table III

Analyzed Silver in $g/m^2 \times 10^2$ for Various Film-Developer Combinations at Different Densities. Corresponding Covering Power Terms (Density/Silver in g/dm^2) are given in Parentheses.

Film	Developer	Dev. Time	$D_V = 0.50$	$D_V = 1.00$	$D_V = 1.50$
KODAK Pan-X	D-76	4 min	40 (125)	82 (122)	111 (135)
	PZ-143	2 3/4 min	40 (125)	93 (107)	118 (127)
	PZ-21	18 min	41 (122)	92 (109)	124 (121)
	POTA	17 min	44 (114)	102 (98)	158 (95)
KODAK Plus-X	D-76	5 min	50 (100)	107 (94)	137 (109)
	PZ-143	3 3/4 min	57 (88)	132 (76)	171 (88)
	PZ-21	20 min	50 (100)	112 (89)	145 (103)
	POTA	28 min	91 (55)	170 (59)	239 (63)
KODAK Tri-X	D-76	5 1/2 min	71 (70)	132 (76)	162 (93)
	PZ-143	4 1/2 min	75 (67)	168 (60)	205 (73)
	PZ-21	30 min	94 (53)	179 (56)	216 (69)
	POTA	30 min	86 (58)	215 (47)	302 (50)

Hence, POTA development results in a silver image deposit of lower covering power than the other developers with these films. The appearance of this image is illustrated in Figure 39 (also see Figure 30) using photomicrographs of the developed silver pattern at equal exposure and matched mid-scale densities with Tri-X for POTA and PZ-143 developers.

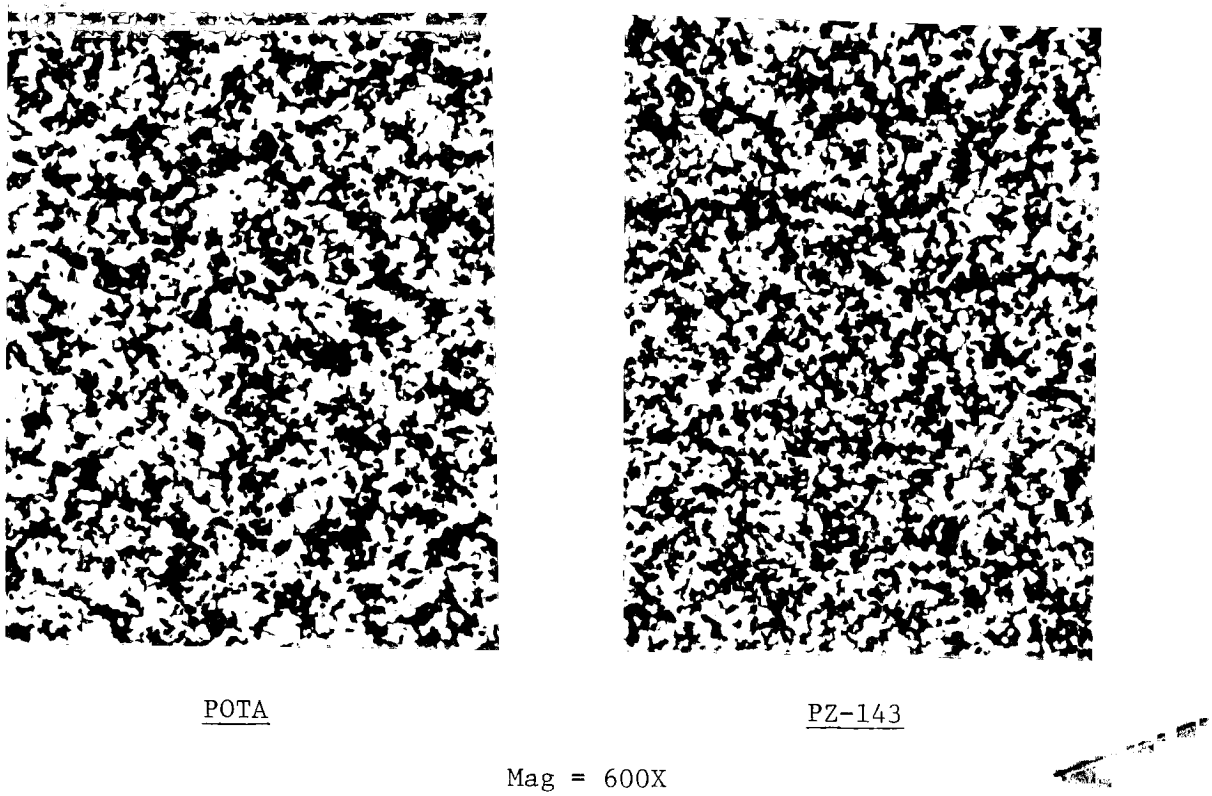

POTA PZ-143

Mag = 600X

Figure 39 - Photomicrographs of the developed silver image obtained with KODAK Tri-X Film with POTA versus PZ-143 at matched exposure and densities (D_V = 0.93).

The much grainer, clumpy silver image deposit obtained with POTA is clearly evident from these photomicrographs. The development inhibition characteristic of POTA results in several areas of the film receiving little development, causing the density to be lower than usual for a given amount of developed silver. This inhibition is not evident with PZ-143 development which employs hydroquinone as a development inhibitor acceptor. The POTA image appears to consist of localized patches of completely developed grains. The PZ-143 image apparently contains a greater number of developed grains, but developed to a lesser extent. The latter type of development fills in the void areas of the film, affording more light-stopping ability (density) for a given developed silver mass.

4(b) Subjective Evaluation

Evaluation of the definition pictures gives qualitative support to the objective acutance-granularity data. With each film, the prints produced from POTA negatives are easily chosen as being the most grainy. The sharpness boost obtained with PZ-143, PZ-21, and POTA over D-76 is also evident with all three films. However, the increase in graininess that accompanies the improved sharpness seems more obvious. With Plus-X and Tri-X, most observers (18 of 20 and 17 of 20, respectively) preferred the D-76 prints. However, with Panatomic-X film, almost half of the observers (9 of 20) preferred some increased sharpness over D-76. Hence with higher speed films like Plus-X and Tri-X, the increase in grain produced by these "high-acutance" developers overwhelms the gain in sharpness, making the trade-off unfavorable. With a lower speed film such as Panatomic-X, the grain-sharpness trade-off may be more beneficial, depending on the personal preferences of the observer. Extrapolating these statements, the trade-off might be of considerable benefit for very fine grain-low speed films. This is evidenced by the fact that POTA is a recommended developer with KODAK Technical Pan Film 2415.[56]

5) MTF Enhancement with Metol and Phenidone

Both low-Metol and Phenidone developers provide increased MTF response (see Appendix C) over conventional developers like D-76 with the three films

studied, as evidenced in Figures 24, 25, and 26. However, the response with increasing frequency is different. Both developers provide low-frequency enhancement, but POTA provides much more enhancement at higher frequencies. This difference in frequency response is due to the difference in enhancement mechanisms between the two developers.

MTF enhancement with low-Metol developers like PZ-21 occurs via fresh active developer attack of highly exposed areas from adjacent areas of lower exposure (exhaustion). Since the Metol concentration is low, development proceeds slowly, and long development times are required. This allows more time for fresh developer attack from the low exposed areas of the sine wave pattern. This is illustrated in the schematic diagram in Figure 40 for a low-frequency situation.

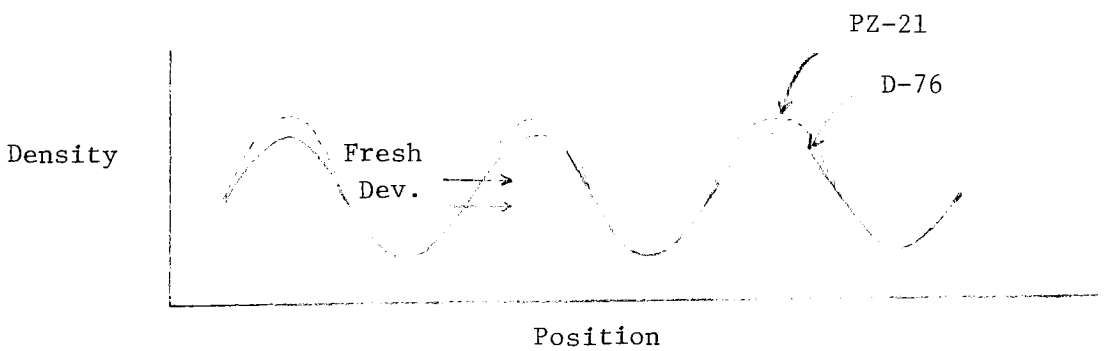

Figure 40 - Schematic Illustration of Low-Frequency MTF Enhancement with Low-Metol Developers.

However, the volume of low exposed area between the high exposed areas is reduced as frequency increases. Hence, less fresh active developer is available for lateral attack of the more heavily exposed areas, as shown in Figure 41.

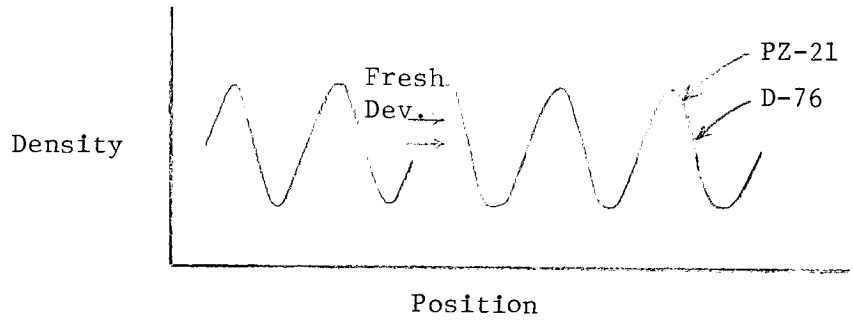

Figure 41 - Schematic Illustration of No High-Frequency MTF Enhancement with Low-Metol Developers.

However, MTF enhancement with POTA development occurs due to the diffusion of development inhibitor (oxidized Phenidone) which is produced imagewise. More inhibitor is released from areas which have received more exposure and development. Presumably, this inhibitor is free to diffuse until it is adsorbed by a neighboring undeveloped grain, usually a short distance away. Hence, high-frequency response is quite plausible and in fact occurs with POTA development, as described in Figure 42.

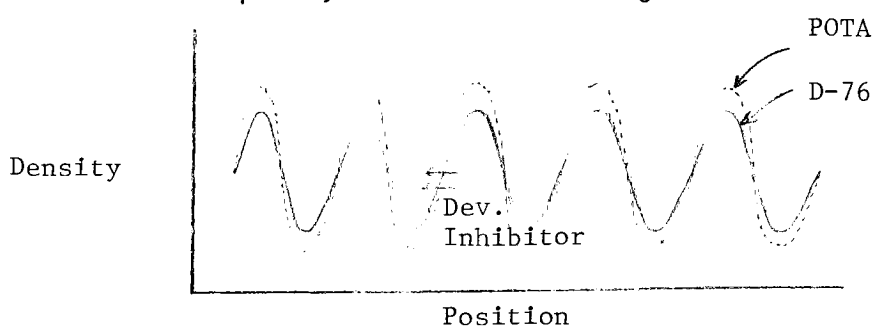

Figure 42 - Schematic Illustration of High-Frequency MTF Enhancement with POTA.

These results also demonstrate that X-ray edge enhancement (1000μ line) represents a low-frequency situation and does not necessarily correlate at high frequencies.

CONCLUSIONS

Increased chemical adjacency effects in black and white photography can be obtained using certain Metol and Phenidone developers. These effects occur in at least four ways:

1) iodide ion inhibition
2) bromide ion inhibition
3) exhaustion of Metol
4) development inhibition by oxidized Phenidone.

Edge effects produced by Metol exhaustion and by Phenidone development are reduced by the addition of hydroquinone, high levels of sodium sulfite, and high fog levels. They are enhanced by moderate increases in pH.

Developers designed to increase adjacency effects also increase granularity. The trade-off between acutance and granularity is approximately linear for the film-developer combinations used. A one CMT unit improvement in acutance was accompanied by a two $10^3\sigma_D/\gamma$ unit increase in granularity, with the exception of POTA, which resulted in excessive granularity. This was likely due to a loss in the number of developed centers.

Metol exhaustion boosts the MTF response at low frequencies, where it is usually most desirable. The greatest MTF gains with Phenidone development are at high frequencies, which are only useful in situations requiring high magnification.

With low-speed films like Panatomic-X, the sharpness increase observed in photographic prints may be beneficial in spite of increased graininess. However, with higher speed films such as Plus-X and Tri-X, the increased grain overwhelms the gain in sharpness, making the trade-off unfavorable.

REFERENCES

1) R. N. Wolfe and R. S. Barrows, Photogr. Soc. Am. J., 13, 554 (1947).

2) G. Haist, "Modern Photographic Processing", Volume I, John Wiley and Sons, Inc., New York, 1979, p. 409.

3) ibid., p. 407.

4) ibid.

5) ibid., p. 414.

6) ibid., p. 413

7) C. E. K. Mees, "The Theory of the Photographic Process", Macmillan Co., New York, 1942, p. 875.

8) Wolfe and Barrows, p. 554.

9) A. Mackie, Brit. J. Photogr., 64, 11 (1917).

10) A. Lockett, Brit. J. Photogr., 65, 67 (1918).

11) A Mackie, Brit. J. Photogr., 55, 193 (1908).

12) R. E. Crowther, Brit. J. Photogr., 63, 883 (1916).

13) W. Falta, Photogr. Ind., 38, 159 (1940).

14) ibid.

15) ibid.

16) R. D. Zakia and H. N. Todd, PMI, 8 (6), 33 (1965).

17) Wolfe and Barrows, p. 554.

18) J. C. Barnes, G. J. Johnston, and W. J. Moretti, Photogr. Sci. and Eng., 8 (6), 312 (1964).

19) T. H. James, "The Theory of the Photographic Process", 4th Edition, Macmillan Publishing Co., Inc., New York, 1977, p. 610.

20) A. Kramer, Mod. Photogr., 32 (10), 28 (1968).

21) W. Beutler, Leica Fotogr., 5, 182 (1953).

22) Haist, p. 419.

23) ibid.

24) ibid.

25) James, p. 609.

26) J. H. Altman and R. W. Henn, Photogr. Sci. and Eng., 5, 129 (1961).

27) Haist, p. 416.

28) ibid.

29) Haist, p. 340.

30) ibid., p. 449.

31) ibid., p. 452.

32) Beutler, p. 184.

33) Haist, p. 381.

34) M. Levy, Photogr. Sci. and Eng., 11, 46 (1967).

35) R. G. Gendron, J. Soc. Mot. Pict. Telev. Eng., 82, 1009 (1973).

36) James, p. 604.

37) Gendron, p. 1009.

38) James, p. 619.

39) E. W. H. Selwyn, Photogr. J., 83, 227 (1943).

40) D. M. Zwick, Personal Communication, October 7, 1982.

41) Haist, p. 419.

42) M. H. Dickerson, Photogr. Eng., 5, 109 (1954).

43) Haist, p. 419.

44) James, p. 609.

45) G. I. P. Levenson, Photogr. J., 89 (B), 13 (1949).

46) James, p. 313.

47) R. G. Willis, Personal Communication, March 8, 1981.

48) Haist, p. 225.

49) Levinson, p. 13.

50) D. G. Dickerson, Personal Communication, January 25, 1981.

51) R. G. Willis, Personal Communication, June 19, 1981.

52) ibid.

53) ibid.

54) A. J. Axford and J. D. Kendall, J. Photogr. Sci., 2, 1 (1954).

55) ibid.

56) Kodak Publication No. P-255.

APPENDICES

APPENDIX A

Calculation of Relative Speed Values

Relative speed values were assigned using a position on the D-log E curve of 0.20 density above base plus fog as the speed point. The speed scale is graduated such that an increase in the relative speed value of 30 units corresponds to a one-stop (0.30 log E) increase in speed. This procedure is outlined in the schematic below:

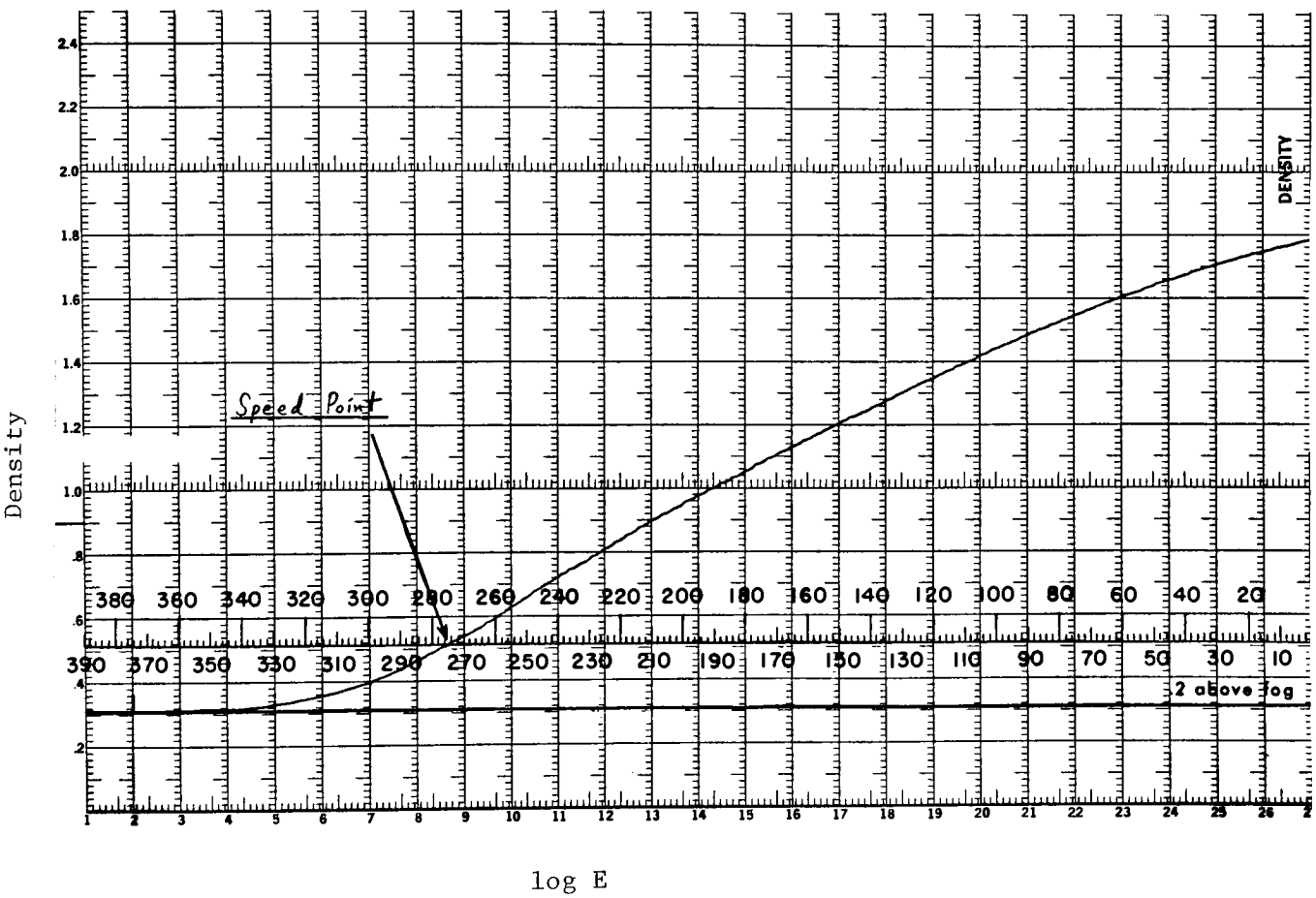

Figure 43 - Method Used to Calculate Relative Speed Values. In this Example the Speed Value is 275.

APPENDIX B

Normalization Procedure for Comparing Edge Densities

Comparisons of adjacency effects among different developers are only legitimate at exactly the same macro density. However, it would obviously be a difficult task to attempt to achieve this in practice with the number of different developers used in these experiments. For this reason, a simple normalization procedure is used to make these comparisons valid yet practical.

An arbitrary value of 1.50 was chosen for macro density. Large adjacency effects are possible at this macro density making differences among developers readily noticeable. The "net edge density" at a macro density of 1.50 was obtained in the following manner. First, the closest macro densities above and below 1.50 along with their corresponding edge densities were determined from the Density versus Development Time plots. Then linear interpolation was used to arrive at an edge density value corresponding to the 1.50 macro density. This edge density minus 1.50 yields the "net edge density" value used to illustrate results. This procedure is described in Figure 44.

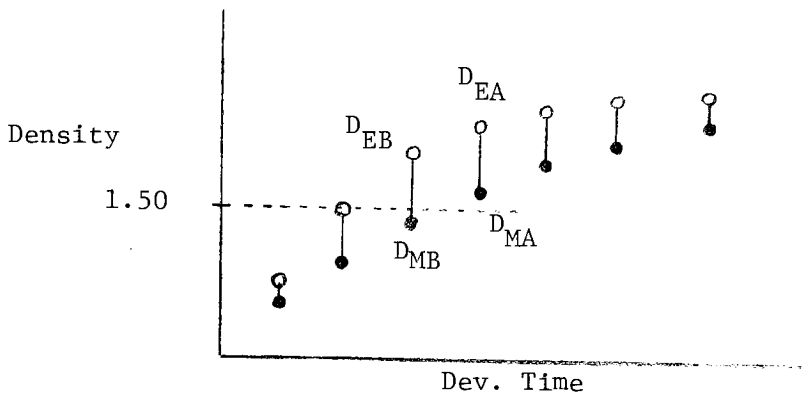

Figure 44 - Edge Density Normalization Procedure.

D_{MB} = closest macro density below 1.50.

D_{MA} = closest macro density above 1.50.

D_{EB} = edge density corresponding to D_{MB}.

D_{EA} = edge density corresponcing to D_{MA}.

The "net edge density" NED is obtained by the following relationship:

$$NED = \left[\left(\frac{D_{MA} - 1.50}{D_{MA} - D_{MB}} \right) X \, (D_{EA} - D_{EB}) + D_{EB} \right] - 1.50$$

APPENDIX C

Calculation of MTF curves and CMT Acutance Values[36,37]

MTF curves and corresponding CMT acutance values were obtained for certain film-developer combinations. These measurements were provided by the Materials Coating and Engineering Division of the Kodak Research Laboratories.

MTF measurements were obtained by exposing the film using a target which consists of a series of sine wave patterns of increasing frequency. Exposure conditions were chosen to achieve a mid-scale density on the corresponding D-log E curve. A 35% modulation target was used.

The resulting density profile of the processed film strips is the physical quantity that is measured. It is then used to calculate the altered exposure profile by means of the film's characteristic curve. This is illustrated in Figure 45.

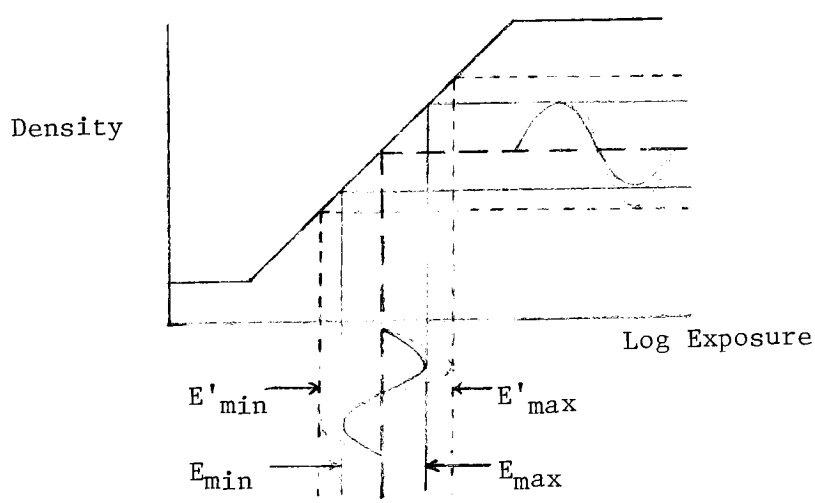

Figure 45 - Sine-wave exposure on a negative working film.

The solid curve represents the response of a film free of optical losses. The dotted curve represents enhanced film due to chemical adjacency effects.

The input exposure is given by $E(x) = E_o (1 + M \sin 2\pi \upsilon x)$ where E_o is the average exposure, M is the modulation of the input exposure, υ is the spatial frequency, and x is the distance. The modulation, M, is defined by

$$M = E_{max} - E_{min})/(E_{max} + E_{min})$$

where E_{max} and E_{min} are given by the equation for E(x) for sin $2\pi \upsilon x$ equal to 1 and -1, respectively. Due to light scattering in the film and chemical adjacency effects the effective exposure, E'(x), is

$$E'(x) - E_o (1+ M' \sin 2\pi \upsilon x)$$

where M' may be less than, equal to, or greater than M depending on the net results of these opposing effects. By conservation of energy, E_o remains constant. Using the expression for the film's characteristic curve $D = D_f + \gamma \log (E/E_f)$ $E_f \leq E \leq E_m$ where D_f is the fog density and D is the maximum density, the density profile resulting from E'(x) is $D(x) = D_f + \gamma \log (E_o/E_f) + \gamma \log (1 + M' \sin 2\pi \upsilon x)$. The values of the peak and valley of the density profile as given by the above equation are measured by means of a microdensitometer. The following relationships are used to calculate D_{min} and D_{max}

$$D_{max} = D_f + \gamma \log (E_o/E_f) + \gamma \log (1+M')$$
$$D_{min} = D_f + \gamma \log (E_o/E_f) + \gamma \log (1-M')$$

By reflecting the measured values of D_{max} and D_{min} back through the film's characteristic curve, the values of the actual exposures E'_{max} and E'_{min} are determined. The actual exposure modulation, M', is then given by

$$M' = (E'_{max} - E'_{min})/(E'_{max} + E'_{min})$$

The ratio between the actual exposure modulation, M', and the input exposure modulation, M, is defined as the modulation transfer, MT, of the film:

$$MT = M'/M$$

When the above procedure is carried out for a range of spatial frequencies, the resulting relation between MT and frequency is called the modulation transfer function, MTF.

CMT acutance values were calculated from the MTF measurements. This method of measuring acutance is based on the theory that MT factors cascade to give a system MTF. The following relationship is used to obtain the CMT acutance:

$$CMT = 125 - 20 \log_{10} x \ (200/\text{MT curve area system})^2$$

where MTF curve area system =

$$\int_0^\infty [MTF_c\ (u') \times MTF_f\ (u') \times MTF_p\ (u') \times MTF_{so}\ (u')]\ du'$$

where MTF_c, MTF_f, MTF_p, MTF_{so} are equal to the MT factors for the camera lens, the film, the projector lens and the standard observer (human visual system), respectively.

u = spatial frequencies for standard test conditions,

M = frequency magnification factor,

u' = Mu, apatial frequencies at the retina of the viewer,

MTF curve area system = the MTF area of the system curve.

In practice, the limits of integration for the MTF cascade are finite, since system MTF curve values become zero at some finite frequency. The upper limit, n, may be imposed by either the human visual system or by the film. The visual system imposes the cutoff for larger film formats and the film imposes the cutoff for small formats. Since these experiments are concerned with film response, a small format system ($\sim$ 12X magnification) is used. Corresponding RMS granularity measurements and definition pictures were obtained at this same magnification. The MT factors for the camera lens, projector lens, and standard observer are kept constant. Hence, under the above conditions the MT characteristics of the film will be the sole factor contributing to any changes in the CMT value.

APPENDIX D

RMS Granularity Measurement[38]

RMS granularity measurements were also obtained for certain film-developer combinations. These measurements were provided by the Film Technical Services Division of Kodak Park.

A 48 μ scanning aperture was used to obtain a microdensitometer trace of a uniformly exposed and developed are of the film, as shown in Figure 46.

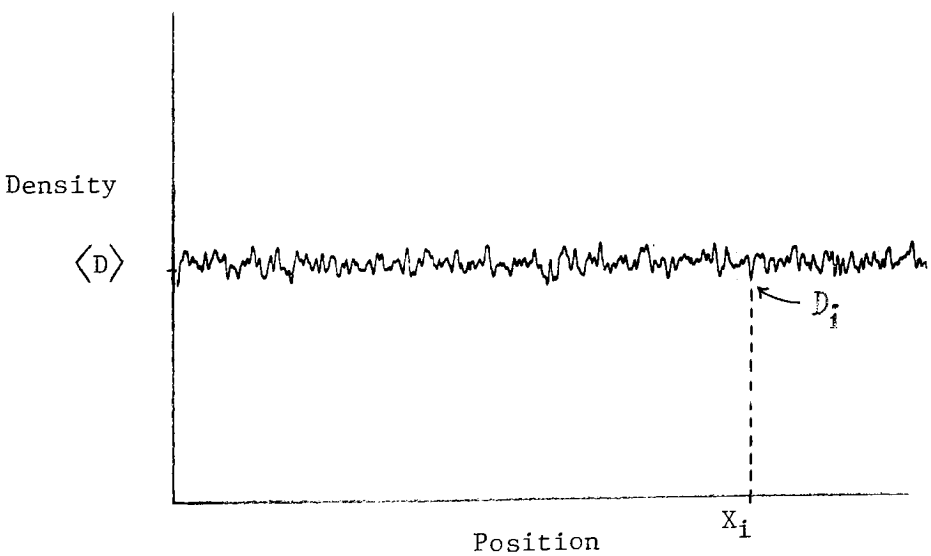

Figure 46 - A microdensitometer trace of KODAK Tri-X Film

Such a microdensitometer trace yields several values of density D_i as a function of position X_i. From these density values, an average Density $\bar{D}$ is obtained. The quantity σ_D, called the root mean square deviation is a measure of uniformity of the developed film sample. It is computed from the data given by the microdensitometer trace using the equation:

$$\sigma_D = \sqrt{\sum_{i=1}^{n} \frac{(D_i - \bar{D})^2}{n-1}}$$

A sample size, n, of density measurements is used to obtain the value of RMS granularity σ_D.

VITA

Paul Zengerle is a photographic chemist at the Kodak Research Laboratories in Rochester, New York. He has attended Rochester Institute of Technology on a part-time basis since 1976.

A Rochester native (born December 16, 1953), he received his Bachelors Degree in Chemistry from the University of Windsor, Ontario, Canada in 1975.

Figure 47 KODAK Panatomic-X Film D-76 Developer

Figure 48 KODAK Panatomic-X Film PZ-143 Developer

Figure 49 KODAK Panatomic-X Film PZ-21 Developer

Figure 50 KODAK Panatomic-X Film POTA Developer

Figure 51 KODAK Plus-X Film D-76 Developer

Figure 52 KODAK Plus-X Film PZ-143 Developer

Figure 53 KODAK Plus-X Film PZ-21 Developer

Figure 54 KODAK Plus-X Film POTA Developer

Figure 55 KODAK Tri-X Film D-76 Developer

Figure 56 KODAK Tri-X Film PZ-143 Developer

Figure 57 KODAK Tri-X Film PZ-21 Developer

Figure 58 KODAK Tri-X Film POTA Developer